doi.org/10.26434/chemrxiv.7388162.v1

Monodisperse Polysarcosine-Based Antibody-Drug Conjugates

Warren Viricel, Guy Fournet, Sabine Beaumel, Emeline Perrial, Sébastien Papot, Charles Dumontet, Benoît Joseph

Submitted date: 27/11/2018 • Posted date: 28/11/2018

Citation information: Viricel, Warren; Fournet, Guy; Beaumel, Sabine; Perrial, Emeline; Papot, Sébastien; Dumontet, Charles; et al. (2018): Monodisperse Polysarcosine-Based Antibody-Drug Conjugates. ChemRxiv. Preprint.

We report the on-resin synthesis of monodisperse (i.e. discrete) polysarcosine compounds and their use as an hydrophobicity masking entity for the construction of highly-loaded homogeneous antibody-drug conjugates (ADC). The polysarcosine-based drug-linker platform described herein improves drug-loading, physicochemical properties, pharmacokinetics and shows excellent potency in vivo.

File list (3)

COMM-Chemrxiv.pdf (572.17 KiB)	view on ChemRxiv • download file
ESI-Chemrxiv.pdf (689.12 KiB)	view on ChemRxiv • download file
TOC-figure.png (211.18 KiB)	view on ChemRxiv • download file

Monodisperse Polysarcosine-based Antibody-Drug Conjugates

Warren Viricel*[a], Guy Fournet[b], Sabine Beaumel[c], Emeline Perrial[c], Sébastien Papot[d], Charles Dumontet[c], and Benoît Joseph[b]

Abstract: We report the on-resin synthesis of monodisperse (i.e. discrete) polysarcosine compounds and their uses as an hydrophobicity masking entity for the construction of highly-loaded homogeneous antibody-drug conjugates (ADC). The polysarcosine-based drug-linker platform described herein improves drug-loading, physicochemical properties, pharmacokinetics and shows excellent potency in vivo.

Current advances in the antibody-drug conjugates (ADC) field of research arise from the understanding that drug-linker design strongly influences the physicochemical properties of the conjugates.[1–3] Key parameters such as (i) plasmatic stability of the drug-linker[4,5], (ii) Drug-Antibody-Ratio (DAR)[6,7], (iii) conjugation position on the antibody component[8], (iv) overall hydrophobicity[9] and homogeneity[10] of the conjugates dictates their pharmacokinetics (PK), efficacy and tolerability. It has notably been reported that a 2-to-4 cytotoxic payload per antibody ratio (DAR2-4) achieves the optimal balance among pharmacokinetics and potency *in vivo*.[6,7] This observation is a consequence of the increased hydrophobicity of the ADC intrinsically conferred by the highly hydrophobic drug cargo.

In light of these findings, a great emphasis on site-specific bioconjugation technologies aiming to deliver homogeneous DAR2 or DAR4 conjugates is observed in the field and began to translate into the clinic.[2,11,12] These techniques require protein genetic re-engineering and/or the use of one or several coupling enzymes to graft the drug-linker payload to the antibody. As a consequence, their implementation is time-consuming, rather expensive and may prove to be difficult to transpose to large-scale production.

Recently, hydrophilic drug-linker architectures aiming to mask or minimize the apparent hydrophobicity of the payloads and overcome the DAR2-4 limitation have paved the way to a new generation of highly drug-loaded ADCs.[13] These innovations enables improved physicochemical properties, excellent PK profiles, decreased non-specific uptake, protection against payload metabolism, superior efficacy in low-target expressing tumors and allow the use of moderately potent drugs as ADC payloads.[9,14–18] One beneficial consequence of this approach is the possibility to obtain homogeneous ADCs without site-specific conjugation technologies. Underlying all these observations, it is also admitted that a beneficial correlation exists between the overall hydrophilicity and tolerability of ADCs.[9,19]

Most of the strategies employed in this new class of drug-linker rely on the use of hydrophilic polyethylene glycol (PEG)[20–23], which is to-date the gold standard to improve physicochemical properties of therapeutic agents, but is not exempt of several limitations (non-biodegradable backbone and reported cases of hypersensitivity or accelerated blood clearance).[24,25] Other approaches use hydrophilic stealth polymer carriers as drug-linker platforms, thus providing ADCs reaching DAR10-20.[14,17] The main drawback of this approach is the extreme polydispersity of the final ADCs, arising from the polydisperse nature of the polymer-linker and the heterogeneous coupling procedure to the antibody.

Polysarcosine (PSAR) or poly(N-methyl-glycine), a polypeptoid based on the endogenous sarcosine aminoacid, is a rather underexplored biocompatible and biodegradable polymer that has been employed as an hydrophilic block in copolymers for nanosized drug delivery systems[26], as an antifouling polymer for surface modification[27] and in fluorophore-conjugate constructs for imaging purposes.[28]

In the present work we envisioned the use of PSAR as an hydrophobicity masking entity that would be embedded into an ADC drug-linker platform, ultimately providing highly-loaded ADCs having improved physicochemical and pharmacological properties. To date, only polydisperse polymeric PSAR is available, as it is accessed *via* a condensative ring-opening polymerization reaction.[29] These polydisperse PSAR are suboptimal in the context of ADCs, where developing a drug-linker platform with absolute chemical homogeneity is highly preferable. Such a platform would provide chemically homogeneous ADCs sharing the exact same pharmacological properties (PK and efficacy), would be more straightforward to characterize and would allow greater control of the reproducibility of the manufacturing process.

As a result, we decided to access monodisperse (*i.e.* discrete) PSAR oligomers by a submonomer solid-phase synthesis method (Scheme 1).[30] Alternating acylation steps by bromoacetic acid and diisopropylcarbodiimide with nucleophilic displacement steps by methylamine afforded monodisperse polysarcosine oligomers with excellent crude purity (Scheme S1 and S2). One of the major difficulties faced during this synthesis was the observation that an almost quantitative diketopiperazine formation occurred at the dimeric stage, despite the use of a

[a] Dr. W. Viricel
Mablink Bioscience SA, 14 rue Waldeck Rousseau, 69006 Lyon, France
E-mail: w.viricel@mablink.com
[b] Dr. G. Fournet, Dr. B. Joseph
Institut de Chimie et Biochimie Moléculaires et Supramoléculaires, UMR CNRS 5246, University of Lyon 1, 1 rue Victor Grignard, 69622 Villeurbanne, France
[c] S. Beaumel, E. Perrial, Dr. C. Dumontet
Centre de Recherche en Cancérologie de Lyon, INSERM 1052, CNRS 5286, University of Lyon 1, 8 avenue Rockefeller, 69008 Lyon, France
[d] Dr. S. Papot
Institut de Chimie des Milieux et des Matériaux de Poitiers (IC2MP), Université de Poitiers, UMR-CNRS 7285, Groupe "Systèmes Moléculaires Programmés", 4 rue Michel Brunet, TSA 51106, F-86073 Poitiers, France

Supporting information for this article is given via a link at the end of the document.

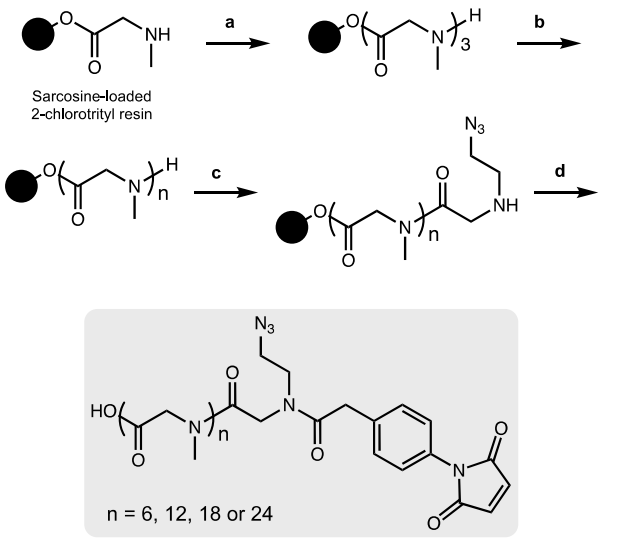

Scheme 1. On-resin synthesis of monodisperse side-functionalized polysarcosine oligomers. (a) Fmoc-Sar-Sar-OH, HATU, DIPEA, DMF then piperidine/DMF. (b) bromoacetic acid (BAA), diisopropylcarbodiimide (DIC), DMF then methylamine in water. This step is repeated until the desired oligomer length is obtained. (c) BAA, DIC, DMF then 2-azidoethan-1-amine, DMF. (d) 4-maleimidophenylacetic acid, COMU, DIPEA, DMF then TFA, CH_2Cl_2.

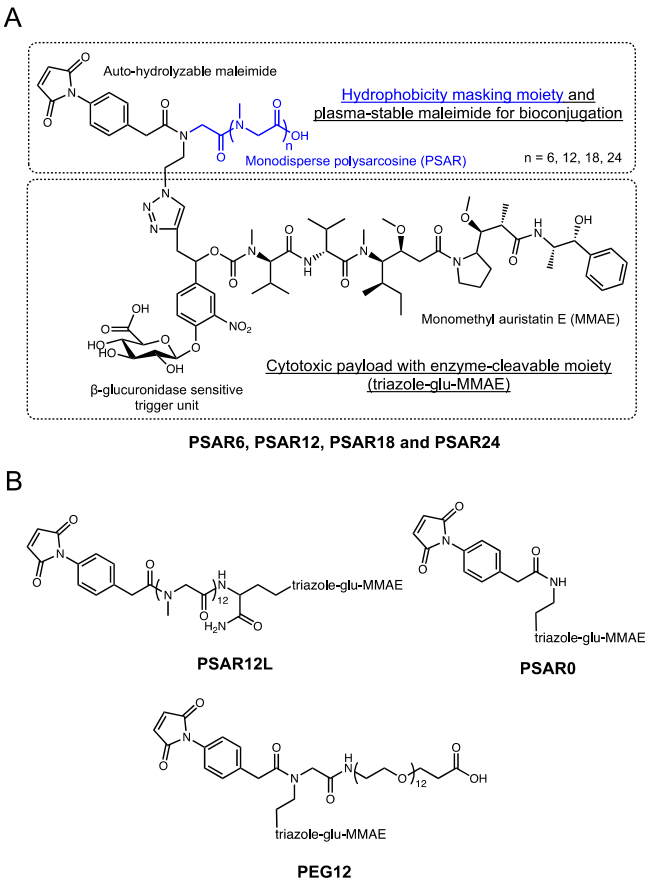

Figure 1. (A) Structure of the polysarcosine-based drug-linker platform. (B) Structures of the negative control drug-linkers used in this study. See supplementary information for detailed chemical synthetic procedures.

2-chlorotrityl solid support (Scheme S3).[31] This was avoided by adding the second and third sarcosine residues as a dipeptoid unit. The PSAR strands were then functionalized with an azide group for subsequent grafting of a cytotoxic payload and terminated with a maleimide reactive moiety for final coupling to the antibody.

To support our proof-of-concept study, a family of PSAR-based drug-linkers was synthesized (Figure 1A and S4-9). We used a β-glucuronidase sensitive trigger associated with potent cytotoxic monomethyl auristatin E (MMAE) as the payload unit.[32,33] Length of the PSAR hydrophobicity masking moiety was incremented from 6 to 24 monomer units, to investigate its effects on physicochemical and pharmacological properties of the resulting ADCs. The linker architecture was optimized in such a way that the hydrophobic payload was the closest as possible to the antibody and the shielding PSAR moiety was in an orthogonal orientation to the payload.[9] An auto-hydrolyzable aryl-maleimide was used to prevent premature deconjugation of the linker-drug in plasma.[34,35]

Control drug-linkers were also synthesized (Figure 1B and S7-9). **PSAR12L** aimed to assess the impact of linker architecture (orthogonal *versus* linear PSAR placement) whereas **PSAR0** lacks PSAR hydrophobicity masking moiety. **PEG12** incorporates PEG instead of PSAR in order to make a side-by-side comparison of the two hydrophobicity masking entities.

Homogeneous DAR8 conjugates based on clinically validated antibody trastuzumab (anti-HER2 mAb) were produced (Figure 2A and S11-14). mAb interchain disulfide bonds were totally reduced with excess tris(2-carboxyethyl)phosphine hydrochloride (TCEP) and drug-linkers were coupled to the antibody (1.25 molar equivalent linker/mAb cysteine — 30 min incubation time). The resulting ADCs were purified by buffer-exchange using Sephadex™ desalting columns and incubated 48 hours at 37°C to promote complete maleimide hydrolysis.

We were pleased to observe that a significant reduction in hydrophobic interaction chromatography (HIC) retention time was observed for the **ADC-PSAR12** conjugate, compared to its negative control **ADC-PSAR0** (Figure 2B and S13). This result demonstrates that inclusion of PSAR in a parallel orientation to the drug unit was able to promote satisfactory hydrophobicity masking and stealth properties to the final conjugate. Inclusion of PSAR in a linear configuration between the mAb and the drug (**ADC-PSAR12L**) was detrimental to the masking of hydrophobicity, as already observed in previous studies.[9] At equal length (n=12 monomer units), PSAR seems to provide better shielding properties than PEG (**ADC-PSAR12** *versus* **ADC-PEG12**). Albeit providing general distinctions between PSAR/PEG hydrophilic moieties or lack thereof, i*n silico* logD or logS predictions of the drug-linkers were unable to provide insight on the crucial impact of the linker architecture on the final ADC hydrophilicity (Figure S10).

To explore if inclusion of an orthogonal PSAR in the drug-linker structure would improve PK properties and antitumor activity, mice PK and xenograft studies were conducted with **ADC-PSAR12** and **ADC-PSAR0**. Without inclusion of PSAR, a

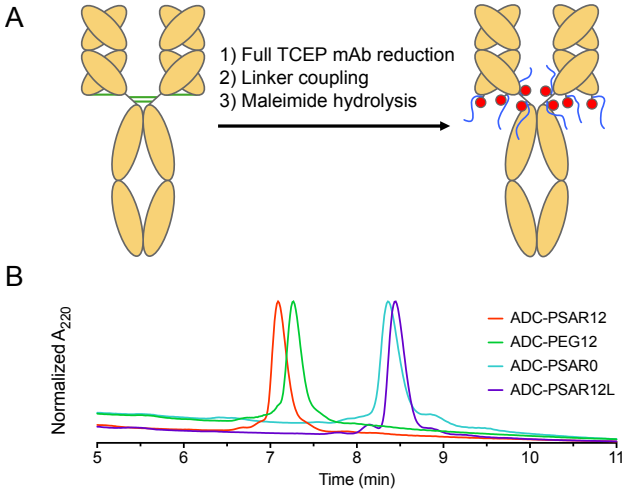

Figure 2. (A) Bioconjugation procedure used to produce homogeneous ADCs with a Drug-Antibody-Ratio (DAR) of 8. (B) Hydrophobic Interaction Chromatography (HIC) profiles of the obtained ADCs. TCEP = Tris(2-carboxyethyl)phosphine hydrochloride.

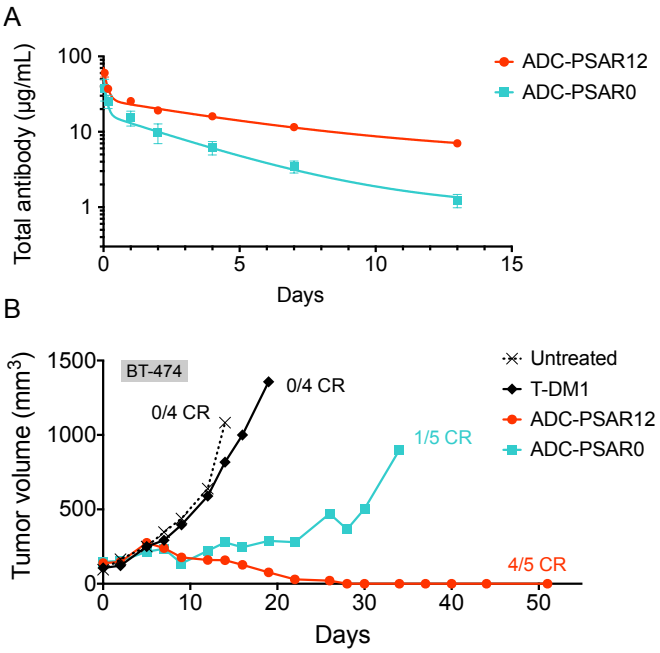

Figure 3. (A) Total ADC pharmacokinetic study in SCID mice after a single intravenous ADC dose of 3 mg/kg. Clearance was 15.8 and 37.6 mL/day/kg respectively for **ADC-PSAR12** and **ADC-PSAR0**, as calculated by two-compartmental model analysis. (B) Antitumor activity in SCID/BT-474 breast cancer model following a single intravenous ADC dose of 3 mg/kg. No body-weight changes were observed during the study. CR = complete remission.

detrimental accelerated plasma clearance was observed, as anticipated for a DAR8 ADC based on a conventional drug-linker (Figure 3A).[6,7] PK profile was restored with the inclusion of the PSAR hydrophobicity masking moiety. Antitumor activity of these two ADCs in a BT-474 breast cancer model was directly correlated with their observed PK behavior (Figure 3B and S15). A single dose of **ADC-PSAR12** at 3 mg/kg was curative whereas **ADC-PSAR0** induced incomplete tumor regressions. At the same dose, the currently approved Trastuzumab-DM1 (Kadcyla®) was only able to promote a negligible tumor growth delay and no cures.

In order to gain some insight on structure-activity relationship of the drug-linkers, more thorough *in vivo* investigations were conducted. The impact of PSAR length on ADC PK properties was investigated in Sprague-Dawley rats, as it has been shown that magnitude of ADC PK differences are more important in rats than in mice.[9] We observed that ADC exposure increased as a function of PSAR length up to 12 monomer residues, eventually reaching a point where further increase of PSAR length had little influence on the clearance rates of the conjugates (Figure 4A, 4B and S16). In accordance with their observed hydrophobicity (Figure 2B), **ADC-PSAR0** and **ADC-PSAR12L** showed unfavorable PK characteristics. These results clearly show that inclusion of an hydrophobicity masking entity in an orthogonal orientation to the drug is mandatory to efficiently restore PK properties. It was also observed that at equal length, PSAR more efficiently improve clearance rates when compared to PEG (respectively 38.9 and 47.3 mL/day/kg for **ADC-PSAR12** and **ADC-PEG12**).

Antitumor activity of these ADCs was investigated in the breast cancer model BT-474, at a single 2.5 mg/kg dose (Figure 4C). Complete tumor regressions were only observed for conjugates having low clearance rates (**ADC-PSAR12** and **ADC-PSAR18**), validating that a 12 monomer PSAR length appears to be an optimized value, at least for this MMAE-based drug-linker (in other experiments conducted in our labs, we observed that the optimized PSAR length is a payload-dependent value that can be more carefully optimized depending on the hydrophobic character and the number of payloads attached to one drug-linker). Interestingly, the **ADC-PSAR24** compound, despite its acceptable clearance profile, had a suboptimal activity. As already observed[20] and because ADC hydrodynamic diameter increases as a function of the hydrophilic shielding entity size, it can be hypothesized that a 24 monomer PSAR length ultimately yields an overlarge and/or hindered conjugate. Such a conjugate may partially impede tumor penetration, interfere with internalization or β-glucuronidase digestion processes and ultimately lead to the observed loss of efficacy.

ADCs having unfavorable (**ADC-PSAR12L**) or suboptimal (**ADC-PSAR6** and **ADC-PEG12**) clearance profiles were only able to promote delayed tumor growth at this dose (Figure 4C). These results confirm the rational orthogonal placement of the PSAR hydrophobicity masking entity and show that, at equal length, PSAR more efficiently improve ADC antitumor activity when compared to PEG (**ADC-PSAR12** *versus* **ADC-PEG12**).

In summary, we herein report the use of monodisperse polysarcosine as an hydrophobicity masking entity for the formulation of high drug-load ADCs having improved physicochemical properties, excellent pharmacokinetic characteristics and exceptional antitumor potencies. Owing to its simplicity, this straightforward approach allows the formulation of optimized plasma-stable homogeneous ADCs without the requirement of hard-to-implement bioconjugation technologies. Our approach can be tailored to obtain ADCs incorporating very

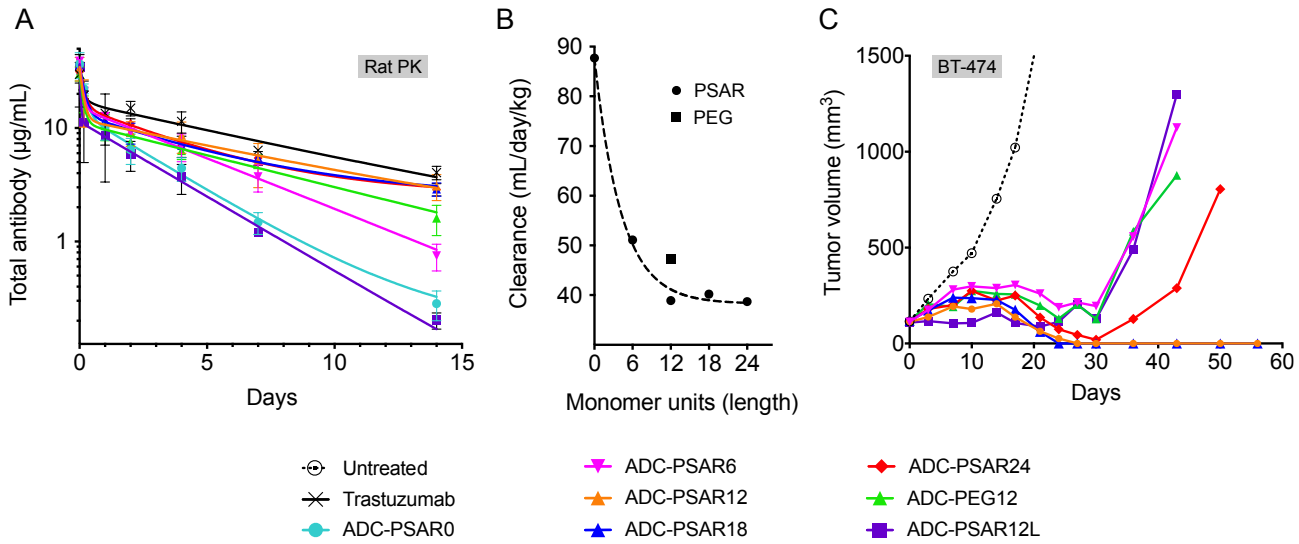

Figure 4. (A) Total ADC pharmacokinetic study in Sprague-Dawley rats after a single intravenous ADC dose of 3 mg/kg and (B) associated clearance rates (two-compartmental model analysis) as a function of the hydrophobicity masking entity length (monomer units). (C) Antitumor activity in SCID/BT-474 breast cancer model following a single intravenous ADC dose of 2.5 mg/kg. No body-weight changes were observed during the study.

hydrophobic payloads known for their aggregation propensity or highly-loaded ADCs bearing conventional or more moderately potent payloads with new mechanisms of action.[1,13] Ongoing efforts focusing on the application of this platform to the preparation of homogeneous DAR8/16 ADCs based on differentiated payloads will be reported elsewhere.

Conflict of interest

Some authors are co-inventors on a patent application related to this work (PCT/EP2018/078949) and are shareholders of Mablink Bioscience SA.

Acknowledgements

The Cancéropôle Lyon Auvergne Rhône-Alpes (CLARA) and the Banque Publique d'Investissement (BPI) are acknowledged for financial support. The authors would like to thank the Antineo team for their contribution and insightful discussions.

Keywords: antibodies • antibody-drug conjugates • bioconjugation • cancer • drug delivery

[1] A. Beck, L. Goetsch, C. Dumontet, N. Corvaïa, *Nat. Rev. Drug Discov.* **2017**, *16*, 315–337.
[2] M. Damelin, Ed. , *Innovations for Next-Generation Antibody-Drug Conjugates*, Humana Press, **2018**.
[3] R. V. J. Chari, M. L. Miller, W. C. Widdison, *Angew. Chem. Int. Ed.* **2014**, *53*, 3796–3827.
[4] Y. Anami, C. M. Yamazaki, W. Xiong, X. Gui, N. Zhang, Z. An, K. Tsuchikama, *Nat. Commun.* **2018**, *9*, 2512.
[5] R. P. Lyon, J. R. Setter, T. D. Bovee, S. O. Doronina, J. H. Hunter, M. E. Anderson, C. L. Balasubramanian, S. M. Duniho, C. I. Leiske, F. Li, et al., *Nat. Biotechnol.* **2014**, *32*, 1059–1062.
[6] K. J. Hamblett, P. D. Senter, D. F. Chace, M. M. C. Sun, J. Lenox, C. G. Cerveny, K. M. Kissler, S. X. Bernhardt, A. K. Kopcha, R. F. Zabinski, et al., *Clin. Cancer Res.* **2004**, *10*, 7063–7070.
[7] X. Sun, J. F. Ponte, N. C. Yoder, R. Laleau, J. Coccia, L. Lanieri, Q. Qiu, R. Wu, E. Hong, M. Bogalhas, et al., *Bioconjug. Chem.* **2017**, *28*, 1371–1381.
[8] B.-Q. Shen, K. Xu, L. Liu, H. Raab, S. Bhakta, M. Kenrick, K. L. Parsons-Reponte, J. Tien, S.-F. Yu, E. Mai, et al., *Nat. Biotechnol.* **2012**, *30*, 184–189.
[9] R. P. Lyon, T. D. Bovee, S. O. Doronina, P. J. Burke, J. H. Hunter, H. D. Neff-LaFord, M. Jonas, M. E. Anderson, J. R. Setter, P. D. Senter, *Nat. Biotechnol.* **2015**, *33*, 733–735.
[10] P. Akkapeddi, S.-A. Azizi, A. M. Freedy, P. M. S. D. Cal, P. M. P. Gois, G. J. L. Bernardes, *Chem. Sci.* **2016**, *7*, 2954–2963.
[11] B. Oller-Salvia, G. Kym, J. W. Chin, *Angew. Chem. Int. Ed.* **2018**, *57*, 2831–2834.
[12] S. S. van Berkel, F. L. van Delft, *Drug Discov. Today Technol.* **2018**, DOI 10.1016/j.ddtec.2018.09.005.
[13] N. Bodyak, A. V. Yurkovetskiy, in *Innov. -Gener. Antib.-Drug Conjug.*, Humana Press, Cham, **2018**, pp. 215–240.
[14] L. Zhang, Y. Fang, J. Kopeček, J. Yang, *Eur. J. Pharm. Sci.* **2017**, *103*, 36–46.
[15] S. V. Govindan, T. M. Cardillo, E. A. Rossi, P. Trisal, W. J. McBride, R. M. Sharkey, D. M. Goldenberg, *Mol. Pharm.* **2015**, *12*, 1836–1847.
[16] Y. Ogitani, T. Aida, K. Hagihara, J. Yamaguchi, C. Ishii, N. Harada, M. Soma, H. Okamoto, M. Oitate, S. Arakawa, et al., *Clin. Cancer Res.* **2016**, *22*, 5097–5108.
[17] A. V. Yurkovetskiy, M. Yin, N. Bodyak, C. A. Stevenson, J. D. Thomas, C. E. Hammond, L. Qin, B. Zhu, D. R. Gumerov, E. Ter-Ovanesyan, et al., *Cancer Res.* **2015**, *75*, 3365–3372.
[18] D. Su, K. R. Kozak, J. Sadowsky, S.-F. Yu, A. Fourie-O'Donohue, C. Nelson, R. Vandlen, R. Ohri, L. Liu, C. Ng, et al., *Bioconjug. Chem.* **2018**, *29*, 1155–1167.
[19] J. M. M. Verkade, M. A. Wijdeven, R. van Geel, B. M. G. Janssen, S. S. van Berkel, F. L. van Delft, *Antibodies* **2018**, *7*, 12.
[20] P. J. Burke, J. Z. Hamilton, S. C. Jeffrey, J. H. Hunter, S. O. Doronina, N. M. Okeley, J. B. Miyamoto, M. E. Anderson, I. J. Stone, M. L. Ulrich, et al., *Mol. Cancer Ther.* **2017**, *16*, 116–123.
[21] M. R. Levengood, X. Zhang, J. H. Hunter, K. K. Emmerton, J. B. Miyamoto, T. S. Lewis, P. D. Senter, *Angew. Chem. Int. Ed.* **2016**, *56*, 733–737.
[22] M. Pabst, W. McDowell, A. Manin, A. Kyle, N. Camper, E. De Juan, V. Parekh, F. Rudge, H. Makwana, T. Kantner, et al., *J. Controlled Release* **2017**, *253*, 160–164.
[23] S.-J. Moon, S. V. Govindan, T. M. Cardillo, C. A. D'Souza, H. J. Hansen, D. M. Goldenberg, *J. Med. Chem.* **2008**, *51*, 6916–6926.
[24] E. M. Pelegri-O'Day, E.-W. Lin, H. D. Maynard, *J. Am. Chem. Soc.* **2014**, *136*, 14323–14332.
[25] P. Zhang, P. Jain, C. Tsao, Z. Yuan, W. Li, B. Li, K. Wu, H.-C. Hung, X. Lin, S. Jiang, *Angew. Chem. Int. Ed.* **2018**, *57*, 7743–7747.
[26] A. Birke, D. Huesmann, A. Kelsch, M. Weilbächer, J. Xie, M. Bros, T.

Bopp, C. Becker, K. Landfester, M. Barz, *Biomacromolecules* **2014**, *15*, 548–557.
[27] K. H. A. Lau, C. Ren, T. S. Sileika, S. H. Park, I. Szleifer, P. B. Messersmith, *Langmuir* **2012**, *28*, 16099–16107.
[28] K. Sano, M. Ohashi, K. Kanazaki, A. Makino, N. Ding, J. Deguchi, Y. Kanada, M. Ono, H. Saji, *Bioconjug. Chem.* **2017**, *28*, 1024–1030.
[29] C. Fetsch, A. Grossmann, L. Holz, J. F. Nawroth, R. Luxenhofer, *Macromolecules* **2011**, *44*, 6746–6758.
[30] R. N. Zuckermann, J. M. Kerr, S. B. H. Kent, W. H. Moos, *J. Am. Chem. Soc.* **1992**, *114*, 10646–10647.
[31] C. Anne, M.-C. Fournié-Zaluski, B. P. Roques, F. Cornille, *Tetrahedron Lett.* **1998**, *39*, 8973–8974.
[32] A. Alouane, R. Labruère, T. Le Saux, F. Schmidt, L. Jullien, *Angew. Chem. Int. Ed.* **2015**, *54*, 7492–7509.
[33] B. Renoux, F. Raes, T. Legigan, E. Péraudeau, B. Eddhif, P. Poinot, I. Tranoy-Opalinski, J. Alsarraf, O. Koniev, S. Kolodych, et al., *Chem. Sci.* **2017**, *8*, 3427–3433.
[34] R. J. Christie, R. Fleming, B. Bezabeh, R. Woods, S. Mao, J. Harper, A. Joseph, Q. Wang, Z.-Q. Xu, H. Wu, et al., *J. Controlled Release* **2015**, *220*, *Part B*, 660–670.
[35] H.-G. Lerchen, S. Wittrock, B. Stelte-Ludwig, A. Sommer, S. Berndt, N. Griebenow, A.-S. Rebstock, S. Johannes, Y. Cancho-Grande, C. Mahlert, et al., *Angew. Chem. Int. Ed.* **2018**, *57*, 15243–15247.

Supplementary Information

Monodisperse Polysarcosine-based Antibody-Drug Conjugates

Warren Viricel[1], Guy Fournet[2], Sabine Beaumel[3], Emeline Perrial[3], Sébastien Papot[4], Charles Dumontet[3] and Benoît Joseph[2]*

[1] Mablink Bioscience SA, 14 rue Waldeck Rousseau, 69006 Lyon, France

[2] Institut de Chimie et Biochimie Moléculaires et Supramoléculaires, UMR CNRS 5246, University of Lyon 1, 1 rue Victor Grignard, 69622 Villeurbanne, France

[3] Centre de Recherche en Cancérologie de Lyon, INSERM 1052, CNRS 5286, University of Lyon 1, 8 avenue Rockefeller, 69008 Lyon, France

[4] Institut de Chimie des Milieux et des Matériaux de Poitiers (IC2MP), Université de Poitiers, UMR-CNRS 7285, Groupe “Systèmes Moléculaires Programmés”, 4 rue Michel Brunet, TSA 51106, F-86073 Poitiers, France

*Address correspondence to w.viricel@mablink.com

Table of supplementary figures

Table of experimental procedures

Abbreviations

ACN: acetonitrile; AcOH: acetic acid; ADC: Antibody-drug conjugate; BAA: bromoacetic acid; COMU: (1-Cyano-2-ethoxy-2-oxoethylidenaminooxy)dimethylamino-morpholino-carbenium hexafluorophosphate; DAR: Drug-antibody ratio; DCC: N,N-Dicyclohexylcarbodiimide; DCM: dichloromethane; DIC: N,N-Diisopropylcarbodiimide; DIPEA: diisopropylethylamine; DMAP: 4-(Dimethylamino)pyridine; DME : 1,2-dimethoxyethane; DMF: dimethylformamide; DMSO: dimethyl sulfoxide; EDC: N-(3-Dimethylaminopropyl)-N-ethylcarbodiimide hydrochloride; EDTA: ethylenediaminetetraacetic acid; EtOAc: ethyl acetate; EtOH: ethanol; HATU: N-[(Dimethylamino)-1H-1,2,3-triazolo-[4,5-b]pyridin-1-ylmethylene]-N-methylmethanaminium hexafluorophosphate N-oxide; HFIP: 1,1,1,3,3,3-hexafluoro-2-propanol; HIC: Hydrophobic interaction chromatography; HOBt: 1-Hydroxybenzotriazole; MeOH : methanol; MAL: maleimide; MMAE: Monomethyl Auristatin E; NMP: 1-Methyl-2-pyrrolidinone; PBS : phosphate buffer saline; PE: petroleum ether; PEG: poly(ethyleneglycol); PFP: pentafluorophenol; PK: pharmacokinetics; PSAR: poly(sarcosine); SEC: size exclusion chromatography; TCEP: Tris(2-carboxyethyl)phosphine hydrochloride; TFA: trifluoroacetic acid; THF: tetrahydrofuran.

Scheme S1. Synthesis pathway of the monodisperse side-functionalized polysarcosine oligomers

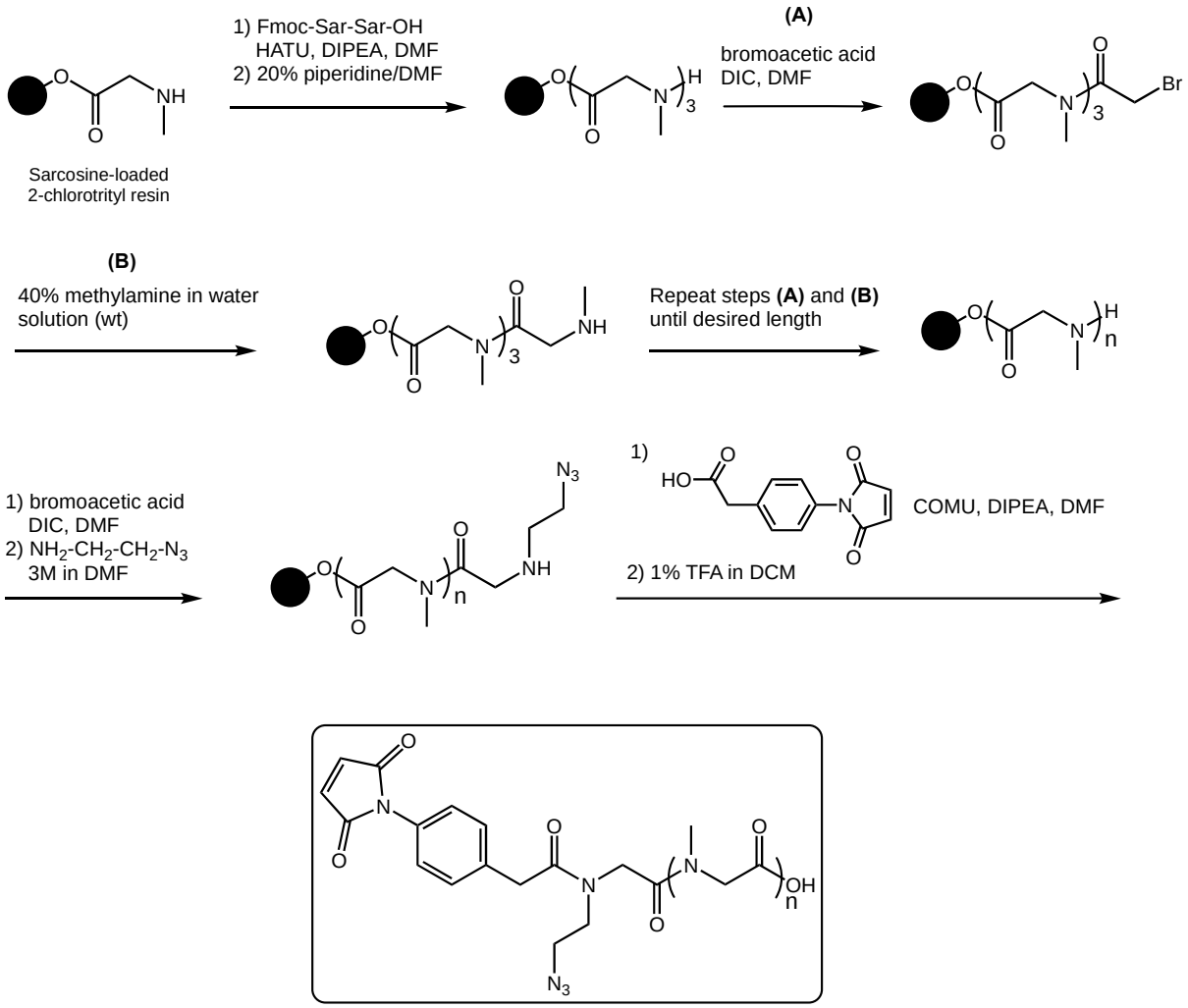

The synthesis and characterization of compounds are further detailed below.

Scheme S2. Synthesis pathway of the monodisperse polysarcosine oligomer used in the negative control PSAR12L drug-linker

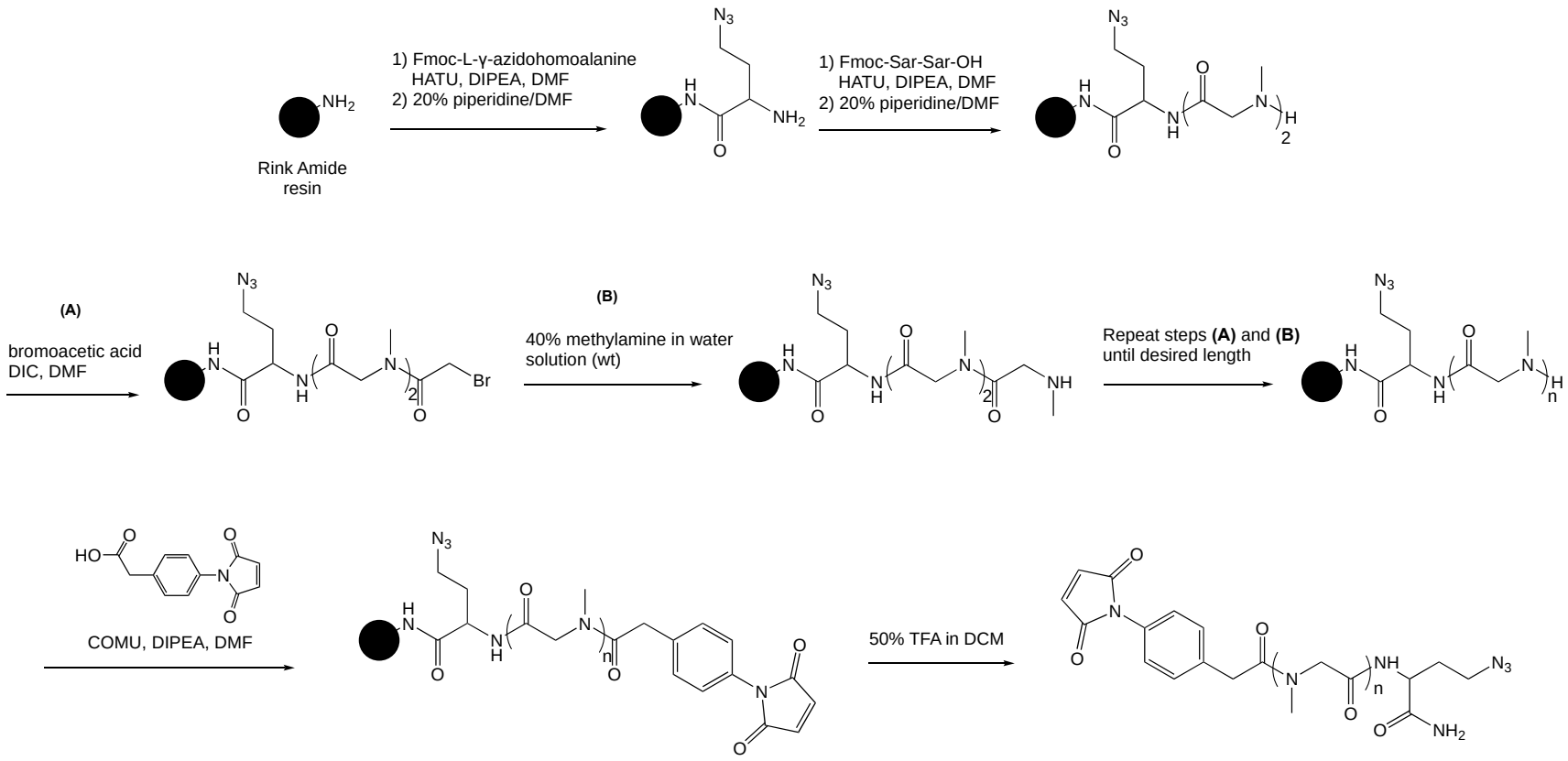

The synthesis and characterization of compounds are further detailed below.

Scheme S3. Detrimental on-resin diketopiperazine formation at the dimeric stage

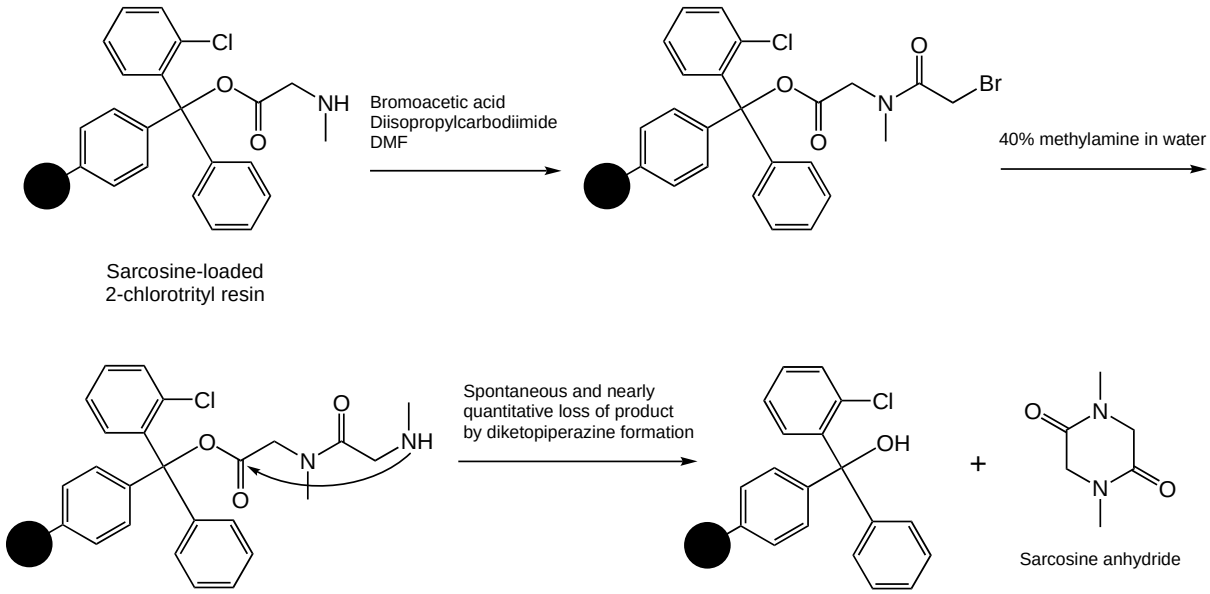

We observed an almost quantitative detrimental diketopiperazine formation at the dimeric stage during PSAR synthesis, as observed by (i) strong colour change of the resin (resin turns orange-brown within minutes), (ii) weight loss of the resin, (iii) yield loss and (iv) detection of sarcosine anhydride by mass spectrometry (m/z $[M+H]^+$ = 143.2) in the eluate after resin drainage. This phenomenon was observed with 2-chlorotrityl solid support (usually known to inhibits diketopiperazine formation because of the steric bulk of the trityl moiety) and Rink amide solid support.

Scheme S4. On-resin synthesis pathway of the side-functionalized PEG used in the negative control drug-linker PEG12

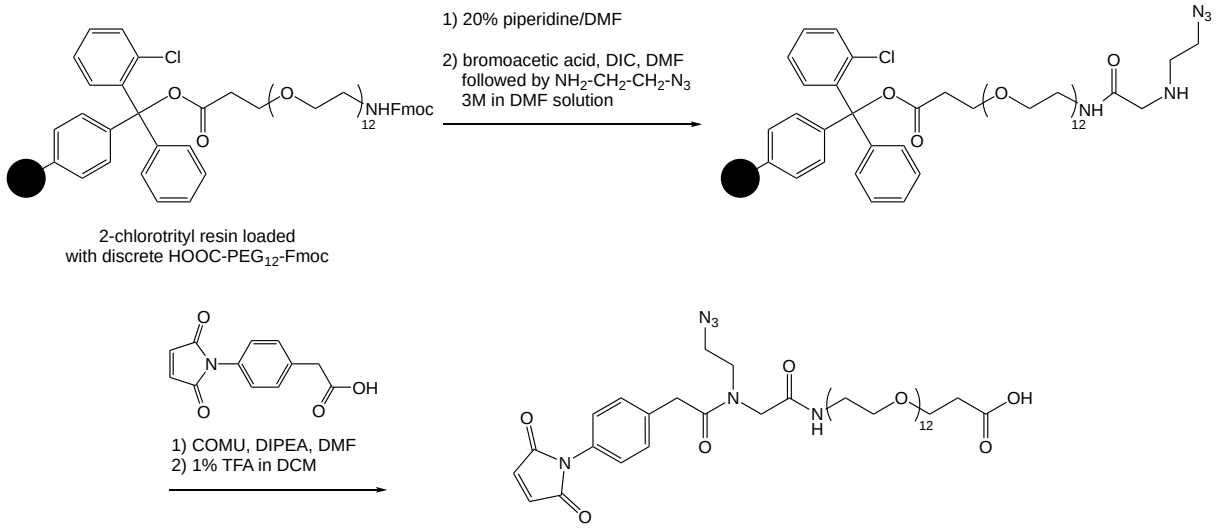

The synthesis and characterization of compounds are further detailed below.

Scheme S5. Synthesis of compound alkyne-glucuronide-MMAE

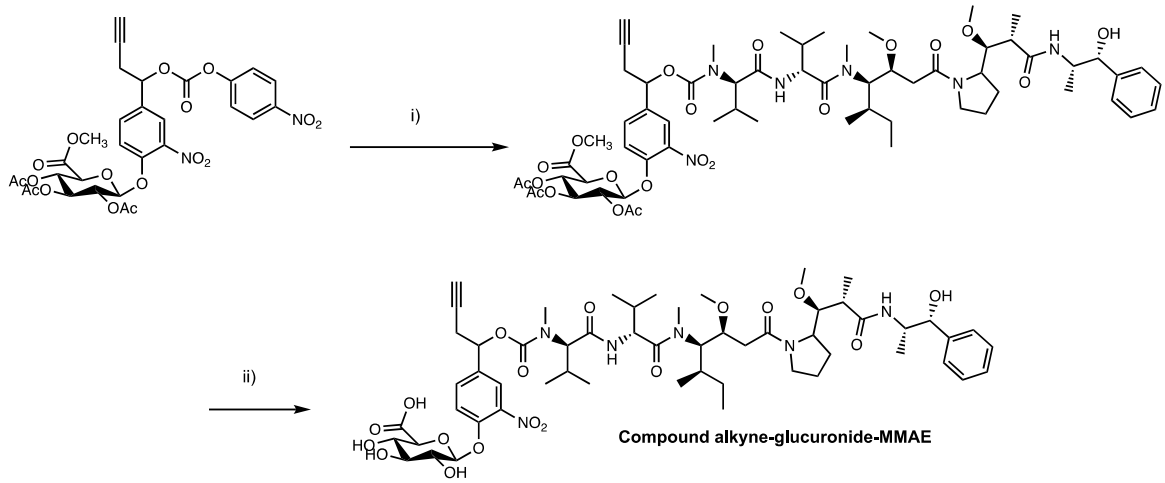

i) Starting carbonate[1], monomethyl auristatin E (MMAE), HOBt, pyridine, DMF, room temp, 16h; ii) LiOH, MeOH/H_2O, 0°C, 60 min.

The synthesis and characterization of compounds are further detailed below.

Scheme S6. Synthesis of polysarcosine-based drug-linkers (PSARn)

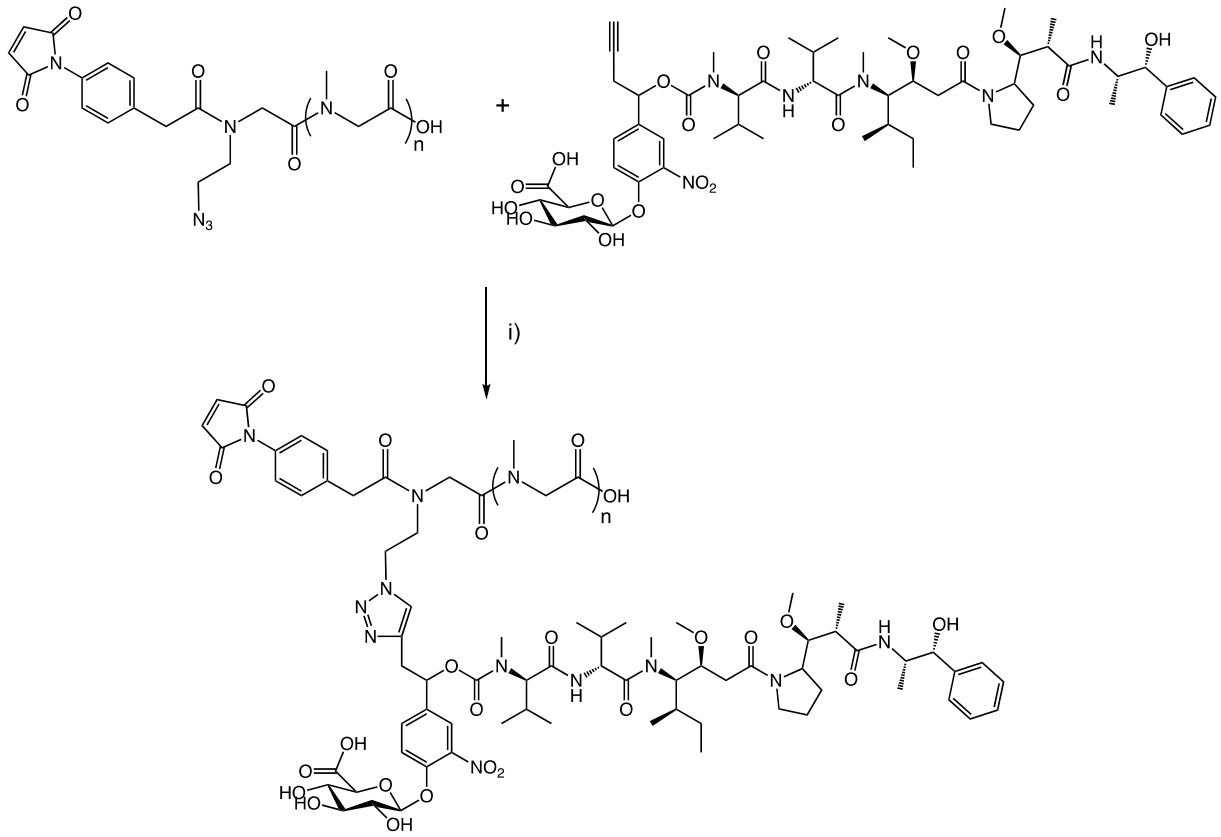

i) tetrakis(acetonitrile)copper(I) hexafluorophosphate, DCM, room temp, 16 hours.

The synthesis and characterization of compounds are further detailed below.

Scheme S7. Synthesis of polyethyleneglycol-based drug-linker (PEG12)

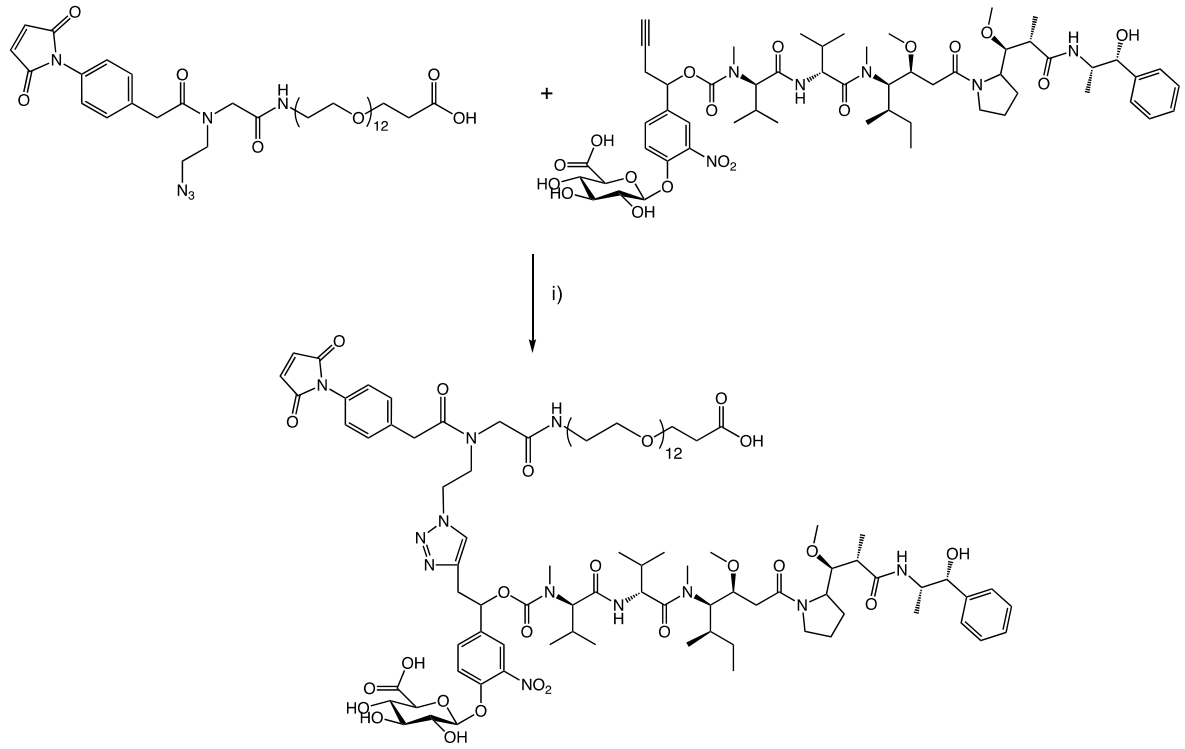

i) tetrakis(acetonitrile)copper(I) hexafluorophosphate, NMP/DCM (2:1 v/v), room temp, 16 hours.

The synthesis and characterization of compounds are further detailed below.

Scheme S8. Synthesis of linear negative control linker (PSAR12L)

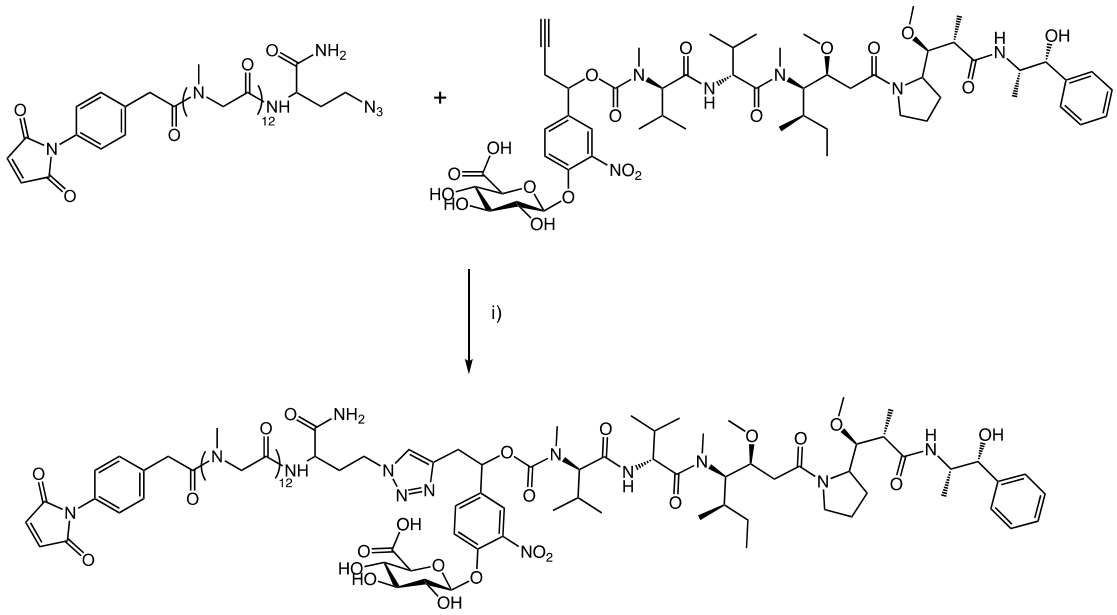

i) tetrakis(acetonitrile)copper(I) hexafluorophosphate, NMP/DCM (2:1 v/v), room temp, 16 hours.

The synthesis and characterization of compounds are further detailed below.

Scheme S9. Synthesis of negative control linker lacking hydrophobicity masking moiety (PSAR0)

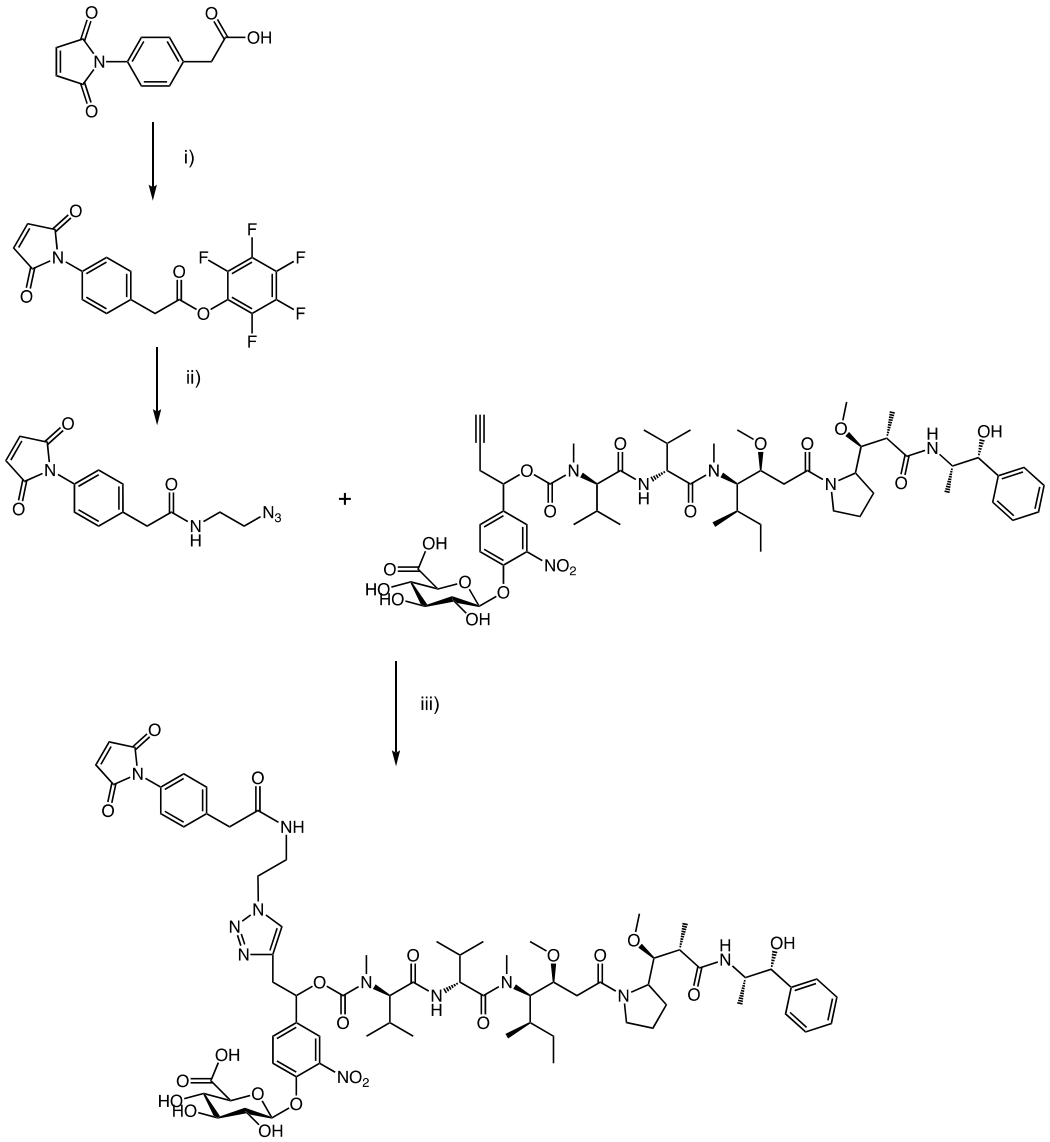

i) DCC, pentafluorophenol, DME, room temp, 2h; ii) NH_2-CH_2-CH_2-N_3, DCM, room temp, 1h; iii) tetrakis(acetonitrile)copper(I) hexafluorophosphate, NMP/DCM/ACN (1:1:1 v/v/v), room temp, 16 hours.

The synthesis and characterization of compounds are further detailed below.

Figure S10. *In silico* logD and logS predictions of drug-linkers

Drug-linker	Linker architecture	logD (pH 7.4)	logS (pH 7.4)
PSAR12	Orthogonal	-14.3	21.2
PSAR12L	Linear	-12.0	20.7
PEG12	Orthogonal	-5	14.8
PSAR0	-	-0.1	0.2

In silico predictions of hydrophobicity (logD at pH 7.4) and water solubility (logS at pH 7.4) were calculated using the Chemicalize Online Calculation Platform from ChemAxon Ltd. Negative logD values indicate a hydrophilic, polar character of the tested compound. High logS values correlate with a greater solubility of the compound in water.

In silico calculations confirms that addition of a polar entity (PSAR or PEG) in the drug-linker architecture positively impacts physicochemical properties of the drug linker (increased hydrophilicity and water solubility of PSAR12, PSAR12L and PEG12 *versus* PSAR0). *In silico* data advantageously predict a more hydrophilic and polar character of PSAR *versus* PEG, in accordance with the observed HIC profiles of the final ADCs (PSAR12 *versus* PEG12 drug-linkers). *In silico* data are unable to predict the favourable impact of an orthogonal linker architecture on the final hydrophilicity of the conjugates as opposed to a linear architecture (drug-linkers PSAR12 and PSAR12L share similar logD and logS values).

Figure S11. Structure of ADCs

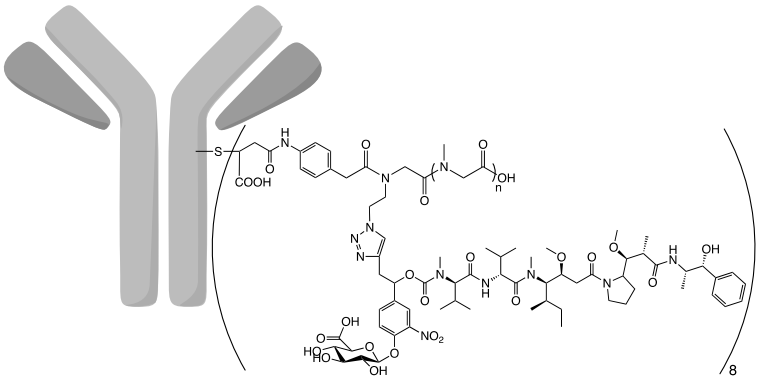

ADC-PSARn :

ADC-PSAR6 (n = 6)
ADC-PSAR12 (n = 12)
ADC-PSAR18 (n = 18)
ADC-PSAR24 (n = 24)

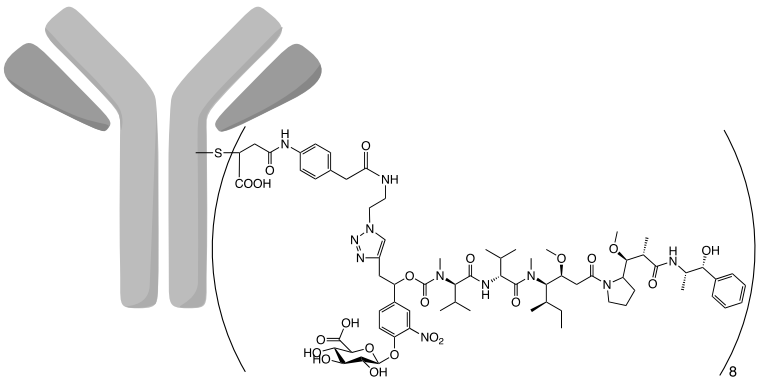

ADC-PSAR0

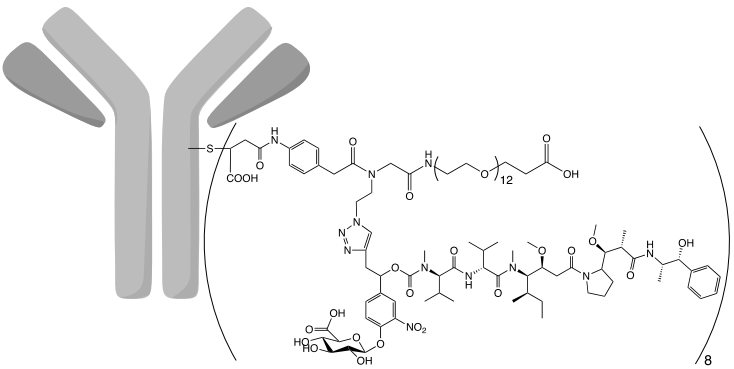

ADC-PEG12

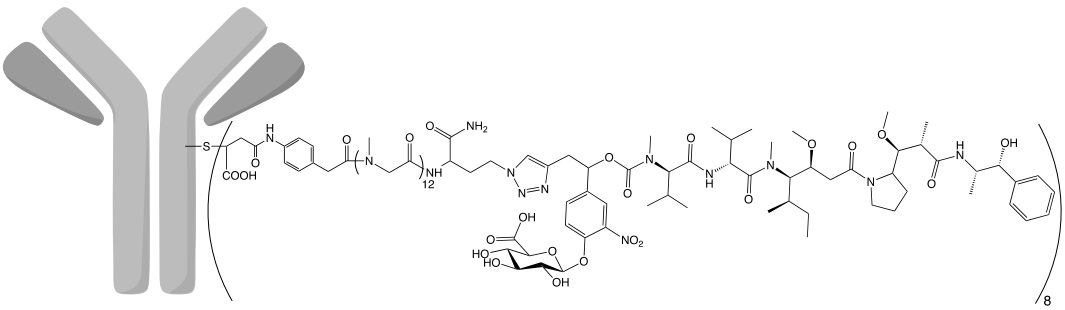

ADC-PSAR12L

Figure S12. RPLC-QToF characterization of ADCs

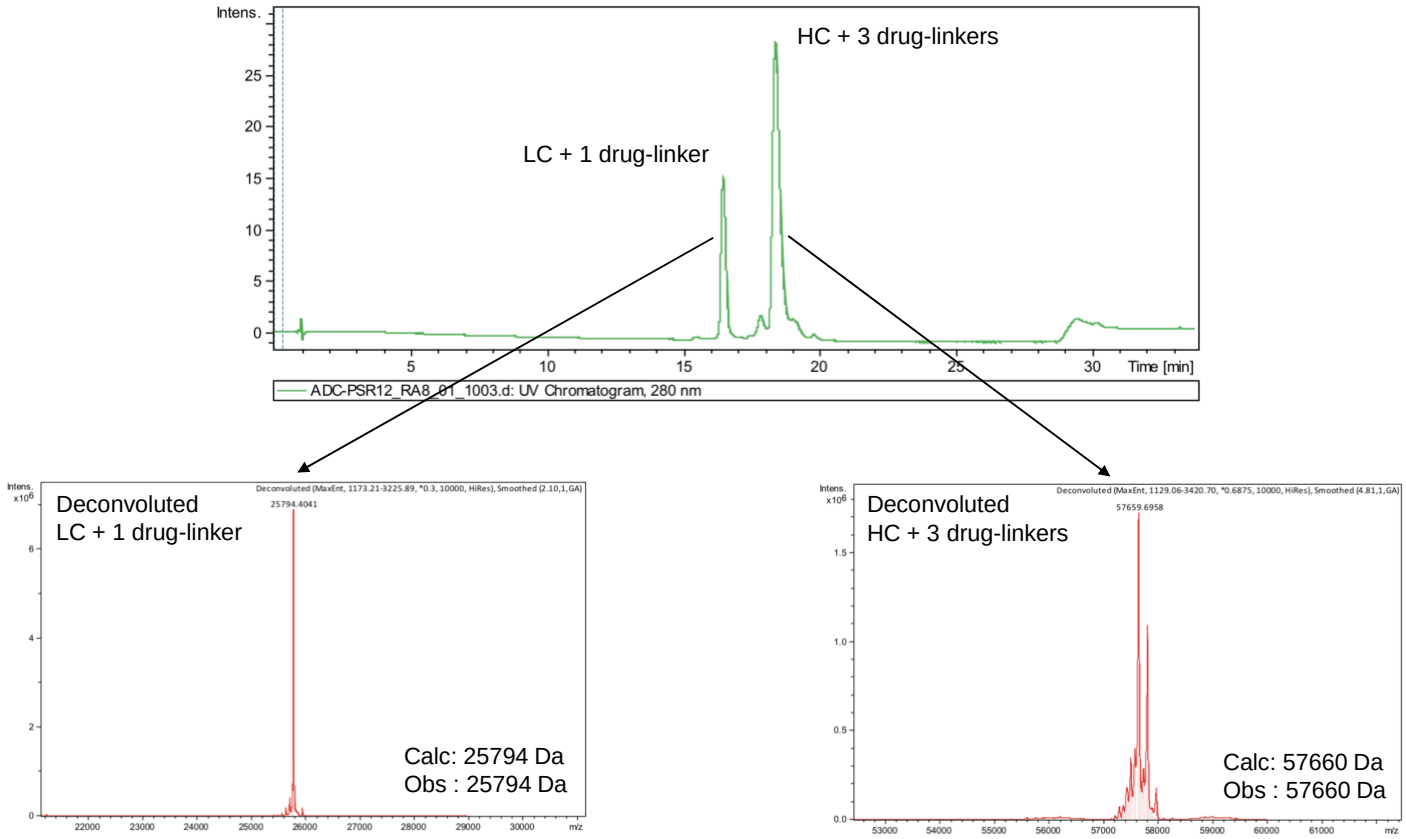

Reverse phase liquid chromatography mass spectrometry (RPLC-QToF) profile of ADC-PSAR12 showed for illustration purposes. Conjugates exhibited one LC-1d (light chain with 1 drug-linker attached) and one HC-3d (heavy chain with 3 drug-linkers attached) absorbance peaks on their denaturing RPLC chromatogram (DAR8 conjugates). For mass spectrometry analysis of the heavy chain of trastuzumab, the major G0F glycoform is reported.

- ADC-PSAR6 (DAR8)
  - Deconvoluted LC-1d Calc: 25368 ; Obs: 25368 / Deconvoluted HC-3d Calc: 56382 ; Obs: 56380
  - Monomeric purity: 99+%
  - HIC retention time: 7.5 min
- ADC-PSAR12 (DAR8)
  - Deconvoluted LC-1d Calc: 25794 ; Obs: 25794 / Deconvoluted HC-3d Calc: 57660 ; Obs: 57660
  - Monomeric purity: 99+%
  - HIC retention time: 7.1 min
- ADC-PSAR18 (DAR8)
  - Deconvoluted LC-1d Calc: 26221 ; Obs: 26221 / Deconvoluted HC-3d Calc: 58939 ; Obs: 58939
  - Monomeric purity: 99+%
  - HIC retention time: 6.8 min
- ADC-PSAR24 (DAR8)
  - Deconvoluted LC-1d Calc: 26647 ; Obs: 26674 / Deconvoluted HC-3d Calc: 60218 ; Obs: 60218
  - Monomeric purity: 99+%
  - HIC retention time: 6.7 min
- ADC-PSAR0 (DAR8)
  - Deconvoluted LC-1d Calc: 24884 ; Obs: 24884 / Deconvoluted HC-3d Calc: 54926 ; Obs: 54926
  - Monomeric purity: 98.5%
  - HIC retention time: 8.4 min
- ADC-PSAR12L (DAR8)
  - Deconvoluted LC-1d Calc: 25793 ; Obs: 25793 / Deconvoluted HC-3d Calc: 57657 ; Obs: 57657
  - Monomeric purity: 99+%
  - HIC retention time: 8.5 min
- ADC-PEG12 (DAR8)
  - Deconvoluted LC-1d Calc: 25541 ; Obs: 25541 / Deconvoluted HC-3d Calc: 56901 ; Obs: 56900
  - Monomeric purity: 99+%
  - HIC retention time: 7.4 min

Figure S13. HIC profiles of polysarcosine-based ADCs

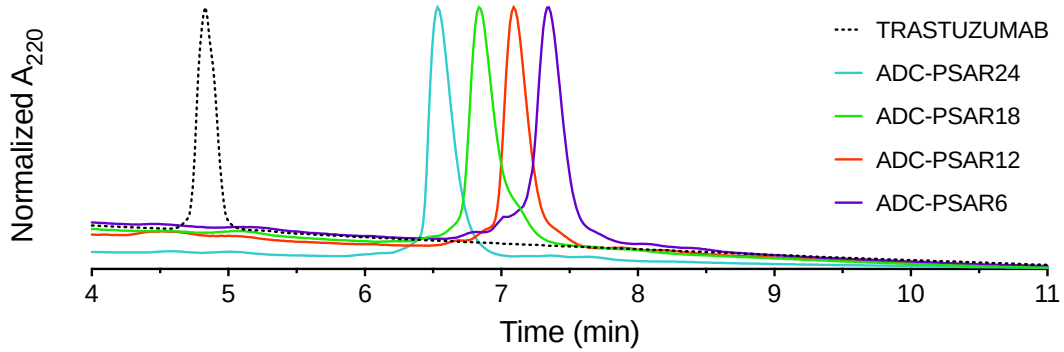

Hydrophobic Interaction Chromatography (HIC) profiles of polysarcosine-based ADCs.

Figure S14. SEC profiles of ADCs

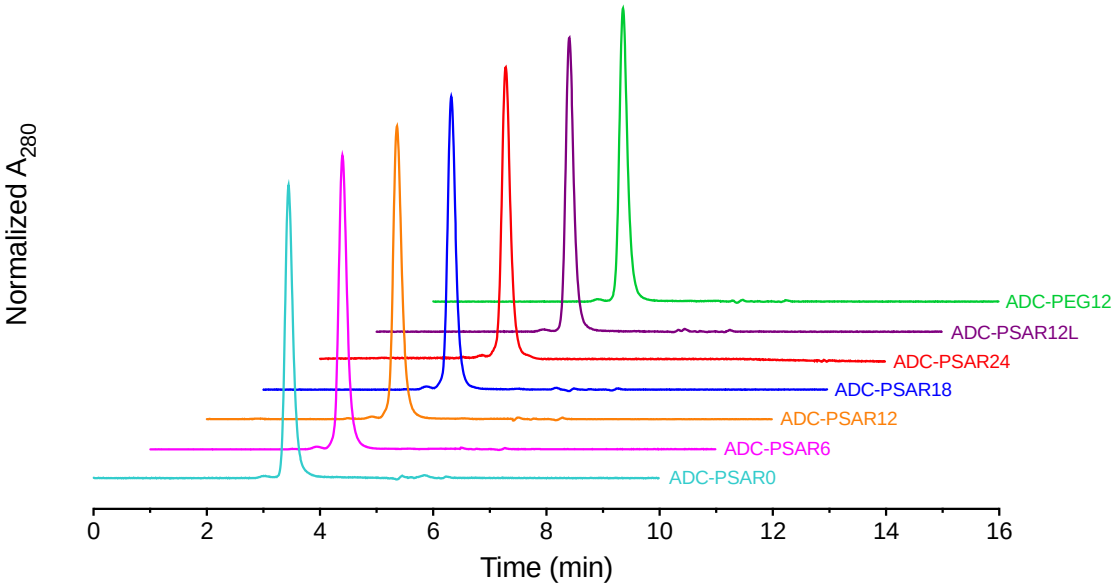

Size exclusion chromatography (SEC) profiles of ADCs used in the present study (<95% monomeric).

Figure S15. Survival curve of the SCID/BT-474 xenograft study

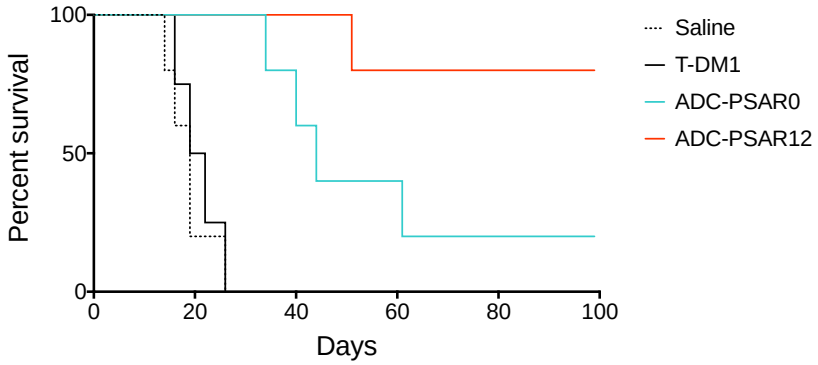

Survival curves of the first SCID/BT-474 xenograft study (Figure 3B). ADCs were injected once intravenously at a dose of 3 mg/kg. No body-weight changes were observed during the study.

Figure S16. Pharmacokinetic parameters (Sprague-Dawley rat PK study)

	TRASTUZUMAB	ADC-PSAR0	ADC-PSAR6	ADC-PSAR12	ADC-PSAR18	ADC-PSAR24	ADC-PEG12	ADC-PSAR12L
Clearance (mL/day/kg)	28.9	87.7	51.1	38.9	40.2	38.7	47.3	103.6
$AUC_{0\text{-}inf}$ (day x µM)	362.2	119.4	204.8	269.4	260.5	270.3	221.3	101.0

Reagents and general methods

All solvents and reagents were obtained from commercial sources (Sigma-Aldrich, Alfa Aesar, Fluorochem, Thermo Fisher, Carbosynth) and used without further purification unless stated otherwise. Anhydrous DMF, DCM and THF were purchased from Sigma-Aldrich. Fmoc-aminoacids and 2-chlorotrityl resin were purchased from Merck. Ramage ChemMatrix® resin was purchased from Sigma-Aldrich. Monodisperse Fmoc-PEG_{12}-COOH was purchased from PurePEG LLC. Monomethyl auristatin E (MMAE) was purchased from DCChemicals. Trastuzumab (Herceptin® IV) and T-DM1 (Kadcyla®) were purchased from Roche. On-resin synthesis was performed in empty SPE plastic tubes equipped with a 20µm polyethylene frit (Sigma-Aldrich). A Titramax 101 platform shaker (Heidolph) was used for agitation. All synthesis yields reported are based upon an initial resin loading of 1.1 mmol/g for 2-chlorotrityl resin and 0.47 mmol/g for Ramage ChemMatrix® resin (extent of labeling indicated by the manufacturers). Unless stated otherwise, all chemical reactions were carried out at room temperature under an inert argon atmosphere.

Liquid nuclear magnetic resonance spectra were recorded on a Bruker Fourier 300HD spectrometer, using residual solvent peak for calibration. Mass spectroscopy analysis has been performed by the Centre Commun de Spectrométrie de Masse (CCSM) of the UMR5246 CNRS institute of the University Claude Bernard Lyon 1.

Normal phase flash chromatography was performed on a Teledyne Isco CombiFlash® Companion® device or Teledyne Isco CombiFlash® Rf200 device using either Interchim (spherical HP 50µm) or Biotage® ZIP® (50µm) silica cartridges. Reverse phase chromatography was performed using Biotage® SNAP Ultra C18 (25µm) cartridges or Interchim PuriFlash RP-AQ (30µm) cartridges. Chemical reactions and compound characterization were respectively monitored and analyzed by thin-layer chromatography using pre-coated 40-63µm silica gel (Macherey-Nagel), HPLC-UV (Agilent 1050) or UHPLC-UV/MS (Thermo UltiMate 3000 UHPLC system equipped with a Bruker Impact II™ Q-ToF mass spectrometer or Agilent 1260 HPLC system equipped with a Bruker MicrOTOF-QII mass spectrometer).

The protocols for experiments in mice and rats were approved by the University of Lyon Animal Ethics Committee. *In vivo* studies were performed at Antineo (Lyon, France — www.antineo.fr).

HPLC methods

HPLC Method 1: Agilent 1050 equipped with DAD detection. Mobile phase A was water and mobile phase B was acetonitrile. Column was an Agilent Zorbax SB-Aq 4.6x150mm 5µm (room temperature). Gradient was 5%B to 95%B in 20 min, followed by a 5 min hold at 95%B. Flow rate was 1.5 mL/min. UV detection was monitored at 214 nm.

HPLC Method 2: Agilent 1050 equipped with DAD detection. Mobile phase A was water and mobile phase B was acetonitrile. Column was an Agilent Zorbax SB-Aq 4.6x150mm 5µm (room temperature). Gradient was 0%B to 50%B in 30 min, followed by a 5 min hold at 50%B. Flow rate was 1.0 mL/min. UV detection was monitored at 214 nm.

HPLC Method 3: Same as HPLC Method 1 but contains 0.1% TFA into the mobile phase A.

HPLC Method 4: Same as HPLC Method 2 but contains 0.1% TFA into the mobile phase A.

Organic chemistry procedures

1. Synthesis of side-functionalized monodisperse polysarcosine oligomers

1.1. Synthesis of Fmoc-Sar-Sar-OH

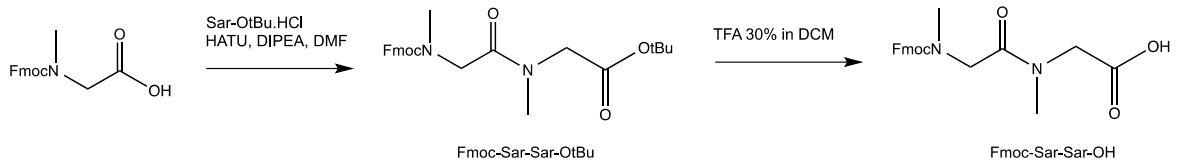

Fmoc-Sar-Sar-OtBu

Fmoc-Sar-Sar-OH

1.1.1. Synthesis of Fmoc-Sar-Sar-OtBu

Fmoc-Sar-OH (2000 mg / 6.42 mmol) and HATU (2443 mg / 6.42 mmol) were dissolved in 28 mL of anhydrous DMF in a round-bottom flask. DIPEA (2491 mg / 19.27 mmol) was added and the mixture was stirred for 3 min at room temperature. Sarcosine tert-butyl ester hydrochloride (1167 mg / 6.42 mmol) was then added and the reaction mixture was stirred at room temperature for 90 min. Volatiles were removed under vacuum and the residue was diluted with water and extracted 3 times with EtOAc. The organic phase was dried over $MgSO_4$, filtered and evaporated under vacuum to afford a solid crude. The crude was taken up in EtOAc/DCM 80:20 (v/v) and white insolubles were removed *via* filtration. The filtrate was purified by chromatography on silica gel (petroleum ether/EtOAc, gradient from 60:40 to 20:80) to afford **Fmoc-Sar-Sar-OtBu** (2310 mg / 82%) as a white solid. HRMS *m/z* (ESI^+): Calc $[M+H]^+$ = 439.2227 ; Exp $[M+H]^+$ = 439.2234 ; Error = -1.5 ppm. HPLC Method 1 retention time = 13.3 min. TLC eluting with 100% EtOAc: Rf=0.8.

1.1.2. Tert-butyl ester removal

Fmoc-Sar-Sar-OtBu (2310 mg / 5.27 mmol) was dissolved in 20 mL of DCM and 8.5 mL of TFA was slowly added. The solution was stirred at room temperature until entire tert-butyl ester deprotection was observed by HPLC (approximately 2 hours). Volatiles were then removed under vacuum and the residue was triturated with diethyl ether to afford **Fmoc-Sar-Sar-OH** (1690 mg / 84%) as a white solid. ^1H NMR (500 MHz, DMSO-d_6, 100°C) δ (ppm) 2.84 (s, 3H), 2.93 (s, 3H), 4.01 (s, 2H), 4.05 (s, 2H), 4.25 (t, *J* = 4.3 Hz, 1H), 4.34 (d, *J* = 6.4 Hz, 2H), 7.33 (t, *J* = 7.4 Hz, 2H), 7.41 (t, *J* = 7.4 Hz, 2H), 7.63

(d, *J* = 7.4 Hz, 2H), 7.85 (d, *J* = 7.5 Hz, 2H). HRMS *m/z* (ESI^+): Calc $[M+H]^+$ = 383.1601 ; Exp $[M+H]^+$ = 383.1602 ; Error = 0.0 ppm. HPLC Method 1 retention time = 6.2 min. TLC eluting with DCM/MeOH 85:15 (v/v): Rf=0.65.

1.2. Synthesis of side-functionalized monodisperse polysarcosine oligomers

1.2.1. Resin loading with Fmoc-Sar-OH

Typically, 1000 mg of 2-chlorotrityl chloride resin beads (100-200 mesh, 1% DVB, 1.1 mmol/g, Novabiochem) were swollen in 10 mL of anhydrous DCM for 10 min. Fmoc-Sar-OH (1.2 eq), previously dissolved in 10 mL of dry DCM, was added onto the resin. DIPEA (5 eq) was added and the reaction vessel was agitated for 2 hours at room temperature. After draining, the resin was washed with DCM (3 times), DMF (2 times), DCM (3 times) and MeOH (2 times). The resin was dried under high vacuum overnight. Substitution level was assessed from the weight gain of the resin and/or from Fmoc cleavage test (absorbance measurement at 301 nm) and was found to be quasi-quantitative (usually 0.95-1.1 mmol/g). Resin was stored at -20°C until further use.

1.2.2. Fmoc-Sar-Sar-OH coupling procedure

Resin was treated with 20% piperidine in DMF (1 mL per 100 mg of resin) for 2 times 15 min at room temperature. The resin was then washed with DMF (4 times) and DCM (4 times). To the resin was added a solution of Fmoc-Sar-Sar-OH (3 eq), HATU (2.85 eq) and DIPEA (6 eq) in DMF (1 mL per 100 mg of resin). The reaction vessel was agitated for 2 hours and the resin was extensively washed with DMF (5 times) and DCM (5 times). The resin was treated with 20% piperidine in DMF (1 mL per 100 mg of resin) for 2 times 15 min at room temperature. The resin was then washed with DMF (4 times) and DCM (4 times). The resin was dried under vacuum and stored at -20°C until further use.

1.2.3. Elongation of polysarcosine

Elongation of the polysarcosine oligomer was performed until the desired length was obtained, by alternating bromoacetylation and amine displacement steps. The bromoacetylation step was performed by adding 10 eq of bromoacetic acid and 13 eq of diisopropylcarbodiimide in DMF (2 mL per 100 mg of resin). The mixture was agitated for 30 min, drained and washed with DMF (4 times). For the amine displacement step, a 40% (wt) methylamine in water solution was added (1.5 mL per 100 mg of resin) and the vessel was shaken for 30 min, drained and washed with DMF (4 times) and DCM (4 times).

1.2.4. Introduction of the azido group

10 eq of bromoacetic acid and 13 eq of diisopropylcarbodiimide in DMF (2 mL per 100 mg of resin) were added onto the resin and the mixture was agitated for 30 min, drained and washed with DMF (4 times). A 3 molar solution of 2-azidoethan-1-amine[2] in DMF was added (1 mL per 100 mg of resin) and the vessel was shaken for 45 min, drained and washed with DMF (4 times) and DCM (4 times).

1.2.5. 4-maleimidophenylacetic acid coupling

To the resin was added a solution of commercially available 4-maleimidophenylacetic acid (5 eq), COMU (4.9 eq) and DIPEA (4.9 eq) in DMF (1 mL per 100 mg of resin). The reaction vessel was agitated for 90 min and the resin was washed with DMF (3 times) and DCM (3 times). Cleavage of the compound of interest from the resin was performed using a 1% TFA in DCM (v/v) solution under agitation for 5 minutes (repeated twice). Resin was filtered and volatiles were removed under reduced pressure to afford a solid crude.

1.2.6. Purification

PSAR compounds were purified on Interchim® RP-AQ (30µm) cartridges. Mobile phase A was water + 0.1% TFA and mobile phase B was acetonitrile + 0.1% TFA. The gradient ranged from 0 to 30% B.

1.2.7. Compounds

Compound Name	Structure	Yield	MS (ESI$^+$)	HPLC Method 4 retention time
PSAR6-N_3-phenyl-MAL (amorphous beige solid)	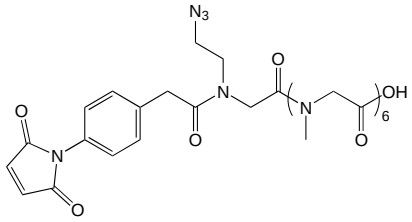	81%	Calc $[M+H]^+$ = 784.3373 Exp $[M+H]^+$ = 784.3342 Error = 3.9 ppm	18.1 min
PSAR12-N_3-phenyl-MAL (beige solid)	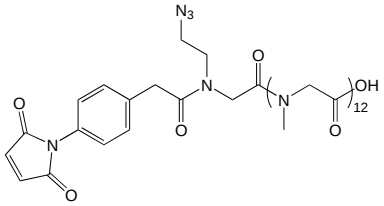	74%	Calc $[M+2H]^{2+}$ = 605.7836 Exp $[M+2H]^{2+}$ = 605.7833 Error = 0.5 ppm	17.2 min
PSAR18-N_3-phenyl-MAL (beige solid)	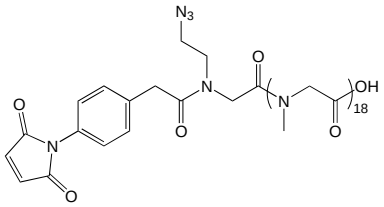	62%	Calc $[M+2H]^{2+}$ = 818.8950 Exp $[M+2H]^{2+}$ = 818.8957 Error = -0.9 ppm	16.4 min
PSAR24-N_3-phenyl-MAL (beige solid)	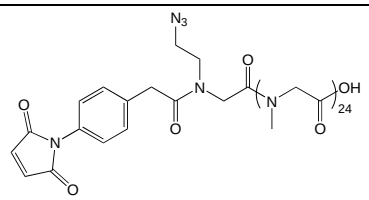	60%	Calc $[M+3H]^{3+}$ = 688.3400 Exp $[M+3H]^{3+}$ = 688.3415 Error = -2.3 ppm	16.5 min

2. Synthesis of monodisperse polysarcosine oligomer used in the negative control PSAR12L drug-linker

2.1. Resin loading with Fmoc-L-γ-azidohomoalanine-OH

Typically, 500 mg of Ramage ChemMatrix® beads (0.47 mmol/g, Sigma-Aldrich) were swollen in 5 mL of DCM for 15 min. Resin was treated with 20% piperidine in DMF (1 mL per 100 mg of resin) for 2 times 15 min at room temperature. The resin was then washed with DMF (4 times) and DCM (4 times). To the resin was added a solution of Fmoc-L-γ-azidohomoalanine-OH (3 eq), HATU (2.9 eq) and DIPEA (6 eq) in DMF (1 mL per 100 mg of resin). The reaction vessel was agitated for 1.5 hours and the resin was extensively washed with DMF (5 times) and DCM (5 times). Unreacted sites were

acetylated using a capping solution made of acetic anhydride/DIPEA/DMF (1:2:3 v/v) (vessel shaken for 30 min). The solution was drained and the resin was washed with DMF (4 times) and DCM (4 times). Resin was treated with 20% piperidine in DMF (1 mL per 100 mg of resin) for 2 times 15 min at room temperature. The resin was then washed with DMF (4 times) and DCM (4 times).

2.2. Fmoc-Sar-Sar-OH coupling procedure

To the resin was added a solution of Fmoc-Sar-Sar-OH (4 eq), HATU (3.9 eq) and DIPEA (8 eq) in DMF (1 mL per 100 mg of resin). The reaction vessel was agitated for 2 hours and the resin was extensively washed with DMF (4 times) and DCM (4 times). The resin was treated with 20% piperidine in DMF (1 mL per 100 mg of resin) for 2 times 15 min at room temperature. The resin was then washed with DMF (4 times) and DCM (4 times).

2.3. Elongation of polysarcosine compounds

Elongation of the polysarcosine oligomer was performed until the desired length was obtained, by alternating bromoacetylation and amine displacement steps, as already described above.

2.4. 4-maleimidophenylacetic acid coupling

4-maleimidophenylacetic acid was coupled following the procedure described above. Cleavage of the compound from the resin was performed using 5 mL of a TFA/DCM (50:50) solution for 30 minutes under agitation at room temperature. The process was repeated once and the pooled filtrates were evaporated under reduced pressure to give a solid crude that was purified on Interchim® RP-AQ (30µm) cartridges as described in the above section.

2.5. Compound

Compound Name	Structure	Yield	MS (ESI+)	HPLC Method 4 retention time
N_3-PSAR12-phenyl-MAL (beige solid)	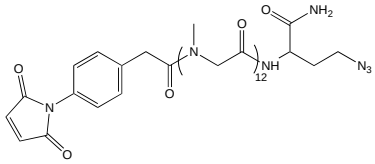	82%	Calc $[M+2H]^{2+}$ = 605.2916 Exp $[M+2H]^{2+}$ = 605.2936 Error = -3.2 ppm	12.5 min

3. Synthesis of side-functionalized PEG used in the negative control drug-linker PEG12

3.1. Resin loading with Fmoc-PEG_{12}-COOH

200 mg of 2-chlorotrityl chloride resin beads (100-200 mesh, 1% DVB, 1.1 mmol/g, Novabiochem) were swollen in 4 mL of anhydrous DCM for 10 min. Fmoc-PEG_{12}-COOH (PurePEG LLC., 1.2 eq), previously dissolved in 2 mL of dry DCM, was added onto the resin. DIPEA (3 eq) was added and the reaction vessel was agitated for 1 hour at room temperature. 300µL of MeOH was added to quench unreacted resin. After 10 min of shaking, the solution was drained and the resin was washed with DMF (3 times) and DCM (3 times). The resin was treated with 20% piperidine in DMF (1 mL per 100 mg of resin) for 2 times 15 min at room temperature. The resin was then washed with DMF (4 times) and DCM (4 times).

3.2. Introduction of the azido group

The bromoacetylation step was performed by adding 10 eq of bromoacetic acid and 13 eq of diisopropylcarbodiimide in DMF (2 mL per 100 mg of resin). The mixture was agitated for 30 min, drained and washed with DMF (4 times). For the amine displacement step, a 3 molar solution of 2-azidoethan-1-amine[2] in DMF was added (1 mL per 100 mg of resin) and the vessel was shaken for 45 min, drained and washed with DMF (4 times) and DCM (4 times).

3.3. 4-maleimidophenylacetic acid coupling

4-maleimidophenylacetic acid was coupled following the procedure described above. Cleavage of the compound of interest from the resin was performed using a 1% TFA in DCM (v/v) solution under agitation for 5 minutes (repeated twice). Resin was filtered and volatiles were removed under reduced pressure to afford an oily crude that was purified on Interchim® RP-AQ (30µm) cartridges as described in the above section.

3.4. Compound

Compound Name	Structure	Yield	MS (ESI$^+$)	HPLC Method 4 retention time
PEG12-N_3-phenyl-MAL (slightly yellow oil)	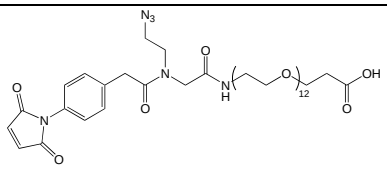	33%	$[M+H]^+$ = 957.5	18.1 min

4. Synthesis of compound alkyne-glucuronide-MMAE

4.1 Step 1

68.4 mg (0.099 mmol) of starting carbonate[1], 71.3 mg (0.099 mmol) of MMAE and 13.5 mg (0.099 mmol) of HOBt were dissolved in 2.4 mL of anhydrous DMF/pyridine (80:20 v/v). After stirring at room temperature for 16 hours, volatiles were evaporated and the residue was purified by chromatography on silica gel (DCM/MeOH, gradient from 98:2 to 95:5) to afford 98 mg (78%) of the protected intermediate as a white solid. $[M+H]^+$ = 1267.6. TLC eluting with DCM/MeOH 95:5 (v/v): Rf=0.7.

4.2 Step 2

110.8 mg (0.087 mmol) of starting material was dissolved in MeOH (10 mL) at 0°C. LiOH monohydrate (36.7 mg / 0.87 mmol) was dissolved in water (1 mL) and was slowly added to the reaction vessel. After stirring at 0°C for 70 min, the mixture was neutralized with acetic acid (68.2 mg / 1.14 mmol) and

concentrated under reduced pressure. The resulting material was taken up in a water/MeOH/DMF solution (1:1:1 v/v) and purified on a 30g Biotage® SNAP Ultra C18 (25µm) cartridge. Mobile phase A was water + 0.1% TFA and mobile phase B was acetonitrile + 0.1% TFA. The gradient ranged from 10 to 60% B. Compound **alkyne-glucuronide-MMAE** (mixture of two diastereoisomers) was obtained as a white solid (95 mg / 96%). LC-HRMS *m/z* (ESI^+): Calc $[M+H]^+$ = 1127.5758 ; Exp $[M+H]^+$ = 1127.5757 ; Error = 0.1 ppm. HPLC Method 3 retention time = 10.3 min.

5. Synthesis of polysarcosine-based drug-linkers (PSARn) by click chemistry

Alkyne-glucuronide-MMAE (1 eq; obtained as described above), PSARn-N_3-phenyl-MAL (1.1 eq; obtained as described above) and tetrakis(acetonitrile)copper(I) hexafluorophosphate (3 eq) were combined in a reaction vessel. DCM was added to reach a final alkyne-glucuronide-MMAE concentration of 12 mM. The reaction was stirred 16 hours at room temperature under argon in the dark. After removal of the volatiles under reduced pressure, the residue was taken up in DMF and purified on a 30g Biotage® SNAP Ultra C18 (25µm) cartridge. Mobile phase A was water + 0.1% TFA and mobile phase B was acetonitrile + 0.1% TFA. The gradient ranged from 10 to 50% B.

Compound **PSAR6** was obtained as a white solid (3.3 mg / 20%). LC-HRMS *m/z* (ESI^+): Calc $[M+2H]^{2+}$ = 955.9566 ; Exp $[M+2H]^{2+}$ = 955.9533 ; Error = 3.4 ppm. HPLC Method 3 retention time = 9.2 min.

Compound **PSAR12** was obtained as a white solid (9.0 mg / 33%). LC-HRMS *m/z* (ESI^+): Calc $[M+2H]^{2+}$ = 1169.0679 ; Exp $[M+2H]^{2+}$ = 1169.0621 ; Error = 4.9 ppm. HPLC Method 3 retention time = 8.7 min.

Compound **PSAR18** was obtained as a white solid (11.5 mg / 40%). LC-HRMS *m/z* (ESI^+): Calc $[M+2H]^{2+}$ = 1382.1792 ; Exp $[M+2H]^{2+}$ = 1382.1803 ; Error = -0.7 ppm. HPLC Method 3 retention time = 8.6 min.

Compound **PSAR24** was obtained as a white solid (15 mg / 44%). LC-HRMS *m/z* (ESI^+): Calc $[M+4Na]^{4+}$ = 820.1309 ; Exp $[M+4Na]^{4+}$ = 820.1324 ; Error = -1.8 ppm. HPLC Method 3 retention time = 8.4 min.

6. Synthesis of polyethyleneglycol-based drug-linker PEG12 by click chemistry

Alkyne-glucuronide-MMAE (obtained as described above) and PEG12-N_3-phenyl-MAL (obtained as described above) were reacted and purified as described in the above section 4, using NMP/DCM (2:1 v/v) as reaction solvent.

Compound **PEG12** was obtained as a slightly yellow oil (10.4 mg / 45%). LC-HRMS *m/z* (ESI^+): Calc $[M+2H]^{2+}$ = 1042.5211 ; Exp $[M+2H]^{2+}$ = 1042.5218 ; Error = -0.7 ppm. HPLC Method 3 retention time = 8.0 min.

7. Synthesis of linear negative control drug-linker PSAR12L by click chemistry

Alkyne-glucuronide-MMAE (obtained as described above) and N_3-PSAR12-phenyl-MAL (obtained as described above) were reacted and purified as described in the above section 4, using NMP/DCM (2:1 v/v) as reaction solvent.

Compound **PSAR12L** was obtained as a white solid (16.0 mg / 39%). LC-HRMS *m/z* (ESI^+): Calc $[M+2H]^{2+}$ = 1168.5759 ; Exp $[M+2H]^{2+}$ = 1168.5792 ; Error = -2.8 ppm. HPLC Method 3 retention time = 6.8 min.

8. Synthesis of negative control drug-linker PSAR0

8.1 Synthesis of perfluorophenyl 2-(4-(2,5-dioxo-2,5-dihydro-1H-pyrrol-1-yl)phenyl)acetate

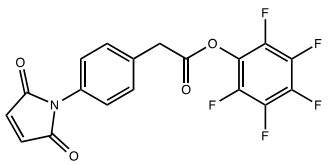

Commercially available 4-maleimidophenylacetic acid (299 mg / 1.29 mmol), DCC (267 mg / 1.29 mmol) and pentafluorophenol (238 mg / 1.29 mmol) were dissolved in 15 mL of anhydrous DME in a reaction vessel. After 2 hours of stirring at room temperature, insolubles were removed by filtration and the filtrate was purified by chromatography on silica gel (petroleum ether/EtOAc, gradient from 80:20 to 20:80) to afford title compound (400 mg / 78%) as a white solid. ^1H NMR (300 MHz, $CDCl_3$) δ (ppm)

4.01 (s, 2H), 6.87 (s, 2H), 7.40 (d, J = 8.7 Hz, 2H), 7.47 (d, J = 8.7 Hz, 2H). HRMS *m/z* (ESI^+): Calc $[M+H]^+$ = 398.0446 ; Exp $[M+H]^+$ = 398.0448 ; Error = -0.4 ppm.

8.2 Synthesis of N-(2-azidoethyl)-2-(4-(2,5-dioxo-2,5-dihydro-1H-pyrrol-1-yl)phenyl)acetamide

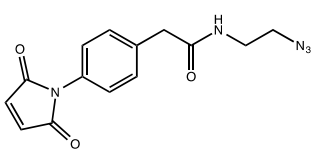

Previous intermediate (78 mg / 0.20 mmol) was dissolved in 1 mL of anhydrous DCM in a reaction vessel. 2-azidoethan-1-amine[2] (33.8 mg / 0.40 mmol) was added and the reaction was stirred 1 hour at room temperature. 1N HCl solution was then added and the mixture was extracted 3 times with DCM. The organic phase was dried over $MgSO_4$, filtered and evaporated under vacuum to afford a solid crude that was purified by chromatography on silica gel (petroleum ether/EtOAc, gradient from 60:40 to 0:100) to afford title compound (18 mg / 31%) as a white solid. MS (ESI^+): $[M+H]^+$ = 300.1 ; HPLC Method 1 retention time = 8.4 min. TLC eluting with 100% EtOAc: Rf=0.65.

8.3 Synthesis of negative control drug-linker PSAR0 by click chemistry

Alkyne-glucuronide-MMAE (obtained as described above) and N-(2-azidoethyl)-2-(4-(2,5-dioxo-2,5-dihydro-1H-pyrrol-1-yl)phenyl)acetamide (obtained as described above) were reacted and purified as described in the above section 4, using ACN/NMP/DCM (1:1:1 v/v/v) as reaction solvent.

Compound **PSAR0** was obtained as an off-white solid (10.3 mg / 48%). LC-HRMS *m/z* (ESI^+): Calc $[M+2H]^{2+}$ = 713.8425 ; Exp $[M+2H]^{2+}$ = 713.8415 ; Error = 1.3 ppm. HPLC Method 3 retention time = 10.2 min.

Preparation of ADCs

A solution of trastuzumab (10 mg/mL in PBS 7.4 + 1 mM EDTA) was treated with 14 molar equivalent of tris(2-carboxyethyl)phosphine (TCEP) for 2 hours at 37°C. The fully reduced antibody was buffer-exchanged with potassium phosphate 100 mM pH 7.4 + 1 mM EDTA by three rounds of dilution/centrifugation using Amicon 30K centrifugal filters device (Merck Millipore). 10 molar equivalents of drug-linker (from a 12 mM DMSO stock solution) was added to the antibody (residual DMSO <10% v/v). The solution was incubated 30 min at room temperature. The conjugate was buffer-exchanged/purified with PBS 7.4 using PD MiniTrap G-25 columns (GE Healthcare) and was sterile-filtered (0.20µm PES filter). Conjugates were diluted at 5 mg/mL with PBS 7.4 and were incubated at 37°C for 48h to promote complete hydrolysis of the succinimidyl moiety. Final protein concentration was assessed spectrophotometrically at 280 nm using a Colibri microvolume spectrometer device (Titertek Berthold). Mass recovery (yield) of the conjugation/purification procedure of was routinely >90%.

Characterization of ADCs

RPLC-QToF

Thermo UltiMate 3000 UHPLC system + Bruker Impact II™ Q-ToF mass spectrometer. Mobile phase A was water + 0.1% formic acid and mobile phase B was acetonitrile + 0.1% formic acid. Column was an Agilent PLRP-S 1000Å 2.1x150mm 8µm (80°C). Gradient was 10%B to 50%B in 25 min. Flow rate was 0.4 mL/min. UV detection was monitored at 280 nm. The Q-ToF mass spectrometer was used in the m/z range 500-3500 (ESI^+). Data were deconvoluted using the MaxEnt algorithm included in the Bruker Compass® software. ADC samples were diluted with H_2O for injection (approx. 1.5 mg/mL final ADC concentration).

SEC

SEC was performed on an Agilent 1050 HPLC system having an extra-column volume below 15µL (equipped with short sections of 0.12mm internal diameter peek tubing and a micro-volume UV flow cell). Column was an Agilent AdvanceBio SEC 300Å 4.6x150mm 2.7µm (maintained at room temperature). Mobile phase was 100 mM sodium phosphate and 200 mM sodium chloride (pH 6.8). 10% acetonitrile (v/v) was added to the mobile phase to minimize secondary hydrophobic interactions with the stationary phase and prevent bacterial growth. Flow rate was 0.35 mL/min. UV detection was monitored at 280 nm.

HIC

Hydrophobic interaction chromatography (HIC) was performed on an Agilent 1050 HPLC system. Column was a Tosoh TSK-GEL BUTYL-NPR 4.6x35mm 2.5 µm (25°C). Mobile phase A was 1.5 M $(NH_4)_2SO_4$ + 25 mM potassium phosphate pH 7.0. Mobile phase B was 25 mM potassium phosphate pH 7.0 + 15% isopropanol (v/v). Linear gradient was 0%B to 100%B in 10 min, followed by a 3 min hold at 100%B. Flow rate was 0.75 mL/min. UV detection was monitored at 220 and 280 nm.

PK studies in mice

ADCs were injected at 3 mg/kg in female SCID mice (4–6 weeks old — Charles River) *via* the tail vein (five animals per group, randomly assigned). Blood was drawn into citrate tubes via retro-orbital bleeding at various time points, processed to plasma and stored at -80°C until analysis. ADC concentration was assessed using a human IgG ELISA kit (Stemcell™ Technologies) according to the manufacturer's protocol. Standard curves of Trastuzumab were used for quantification. Pharmacokinetics parameters (clearance and AUC) were calculated by two-compartmental analysis using Microsoft® Excel® software incorporating PK functions (add-in developed by Usansky et al., Department of Pharmacokinetics and Drug Metabolism, Allergan, Irvine, USA).

PK studies in rats

ADCs were injected at 3 mg/kg in female Sprague-Dawley rats (4–6 weeks old — Charles River) *via* the tail vein (three animals per group, randomly assigned). Blood was drawn into citrate tubes via retro-orbital bleeding at various time points, processed to plasma and stored at -80°C until analysis. ADC concentration was assessed using a human IgG ELISA kit (Stemcell™ Technologies) according to the manufacturer's protocol. Standard curves of Trastuzumab were used for quantification. Pharmacokinetics parameters (clearance and AUC) were calculated by two-compartmental analysis using Microsoft® Excel® software incorporating PK functions (add-in developed by Usansky et al., Department of Pharmacokinetics and Drug Metabolism, Allergan, Irvine, USA).

Xenograft studies

BT-474 breast cancer cells were implanted subcutaneously in female SCID mice (4-5 weeks old). When tumors had grown to approximately 150 mm^3, ADCs were dosed once intravenously (tail vein) at a dose of 3 mg/kg (first study, n = 5 animals/group) or 2.5 mg/kg (second study, n = 6 animals/group). Median tumor growth was assessed by measuring individual tumor volumes every 3-7 days using a caliper device (formula $(L \times W^2)/2$). Mice were sacrificed when the tumor volume exceeded 1000 mm^3. No mice body-weight changes were observed during these studies.

References

1 B. Renoux, F. Raes, T. Legigan, E. Péraudeau, B. Eddhif, P. Poinot, I. Tranoy-Opalinski, J. Alsarraf, O. Koniev, S. Kolodych, S. Lerondel, A. L. Pape, J. Clarhaut and S. Papot, *Chem. Sci.*, 2017, **8**, 3427–3433.

2 Q. Sun, Z. Kang, L. Xue, Y. Shang, Z. Su, H. Sun, Q. Ping, R. Mo and C. Zhang, *J. Am. Chem. Soc.*, 2015, **137**, 6000–6010.

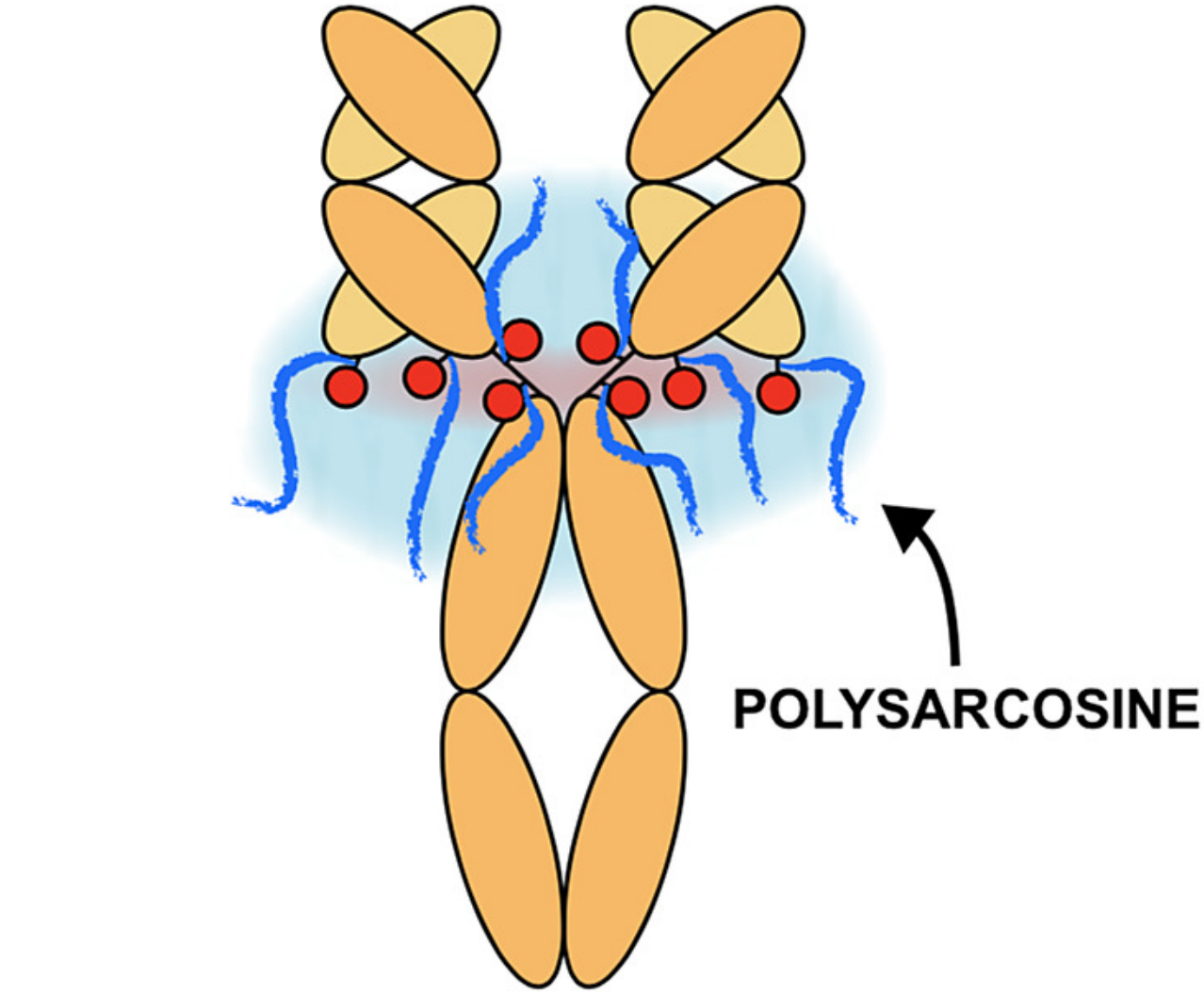

TOC-figure.png (211.18 KiB) view on ChemRxiv • download file